CHAPTER 2 OVERVIEWS AND THEORY

2.1 Glasses [50-52]

2.1.1 Definitions of Glass

The origin of the word glass is the late Latin term *glaesum*, which refers to a lustrous and transparent or translucent body. Glassy substances are also called *vitreous*, originating from the word *vitrum*, again denoting a clear, transparent body. Although, glass became a popular commodity in the growth of civilization, perhaps because of its transparency, luster (or shine), and durability, the understanding of glass no longer requires any of these characteristics to distinguish it current from other substances. Glass can be inorganic (non-carbon-based) as well as organic (carbon-based), and fusion is not the only method to make a glass. Thus, the old American Society for Testing and Materials (ASTM) definition that glass is an inorganic product of fusion which has been cooled to a rigid condition without crystallizing is not appropriate.

Unlike a crystal, glass may not be represented by a simple chemical formula. There are no restrictions with regard to the relative numbers of chemically different atoms other than the fact that the valences and/or coordination requirements may need to be satisfied. Unlike a crystal, glass does not have a sharp melting point when heated. The seemingly rigid solid gradually softens and flows at higher temperatures. At ambient temperatures, however, the viscosity of glass may be sufficiently high that measurable flow does not occur over millennia-certainly not over practical time scales in typical laboratory experiments. It is doubtful that glass windows in building structures of the middle ages have flowed to become thicker at the bottom. Chunks of glass do not have habit planes, nor does glass have identifiable cleavage planes. In the absence of externally applied mechanical, electrical, thermal, magnetic, and gravitational fields, the properties of glass are essentially isotropic like those of a typical liquid.

The isotropic of physical properties makes glasses resemble liquids. It follows that the atomic arrangements in glass must display the long-range order typical of liquids. In order not to be overly restrictive, we are left to define glass as a solid with liquid like structure, a non-crystalline solids or simply as an amorphous solids, with the understanding that the amorphous characteristic here is intended to describe atomic disorder as evidenced by an X-ray diffraction (XRD) analysis; it excludes substances such as "amorphous" powders that may simply be "micro-crystals" and that display more or less sharp peaks in XRD analysis. To get a clearer picture of the fundamentals of glass, we devoted to consideration of the volume-temperature relationship (the v-t diagram) of the glass with respect to a liquid and a crystal.

2.1.2 Type of Glass

The properties of glass can be modified or changed with the addition of other compounds or heat treatment. Since glass was developed on the basis of major commercial used, a large percentage of these are silica-based and more than 99% of glass compositions are oxides. Most glasses contain about 70-72% by weight of silicon dioxide (SiO_2). The most common form of glass is the soda-lime glass, which contains nearly 30% sodium and calcium oxides or carbonates. Pyrex is a borosilicate glass containing about 10 % boric oxide. Lead glass is commonly contains a minimum of 24% lead oxide.

2.1.2.1 Pure silica glass: Chiefly used for its low thermal expansion and high service temperature, and when very pure, for its transparency to a wide range of wavelengths in the electromagnetic spectrum and to sound waves. It also has good chemical, electrical and dielectric resistance. Its disadvantage is the very high temperature needed for manufacture, although it can also be made by hydrolysis of $SiCl_4$; in either case it is expensive. It is used for lightweight mirrors for satellite borne telescopes, laser beam reflectors, special crucibles for the manufacture of pure single crystals of silica for transistors, and as a molecular sieve that lets hydrogen and helium through.

2.1.2.2 Soda-lime glass: The addition of soda (Na_2O) and sometimes potash (K_2O) to silica lowers the softening point by 800-900°C. Lime (CaO) and sometimes magnesia (MgO) and alumina (Al_2O_3) are added to improve the chemical resistance. Electrical properties can vary quite widely with composition. This is the most common of all glasses, used in huge quantities for plate and sheet, containers and lamp bulbs. Crown glass is of this type.

2.1.2.3 Lead glass: Lead oxide reduces the softening point even more than lime and also increases the refractive index and dispersive power. Flint glass for optical purposes and crystal glass for tableware are both lead glass. They are also used for thermometer tube, part of electric lamp and neon-sign tube. Compositions vary widely; a glass of high electrical resistance contains about 25% PbO and 6% or 7% each of Na_2O and K_2O for high refractive index the PbO content may be as much as 65%.

2.1.2.4 Borosilicate glass: Low thermal expansion, about one third that of soda–lime glass, can be made with good chemical resistance and high dielectric strength, and is used where combinations of these are needed. Its high softening temperature makes it harder to work than soda-lime or lead glasses. Used for laboratory glassware, industrial piping, high-temperature thermometer, large telescope mirror, household cooking ware, enclosure for very hot lamp and electric tube of high wattage.

2.1.2.5 Aluminosilicate glass: Another low-expansion, chemically resistant glass that has a higher service temperature than borosilicate glass but is correspondingly harder to fabricate. It is used for high-performance military power tube, traveling wave tube and many applications similar to those of borosilicate glass.

2.1.3 The Enthalpy-Temperature Diagram

Any material which exhibits glass transformation behavior is a glass. Then the glass transformation will be discussed on the basis of either enthalpy or volume versus temperature diagrams, such as that shown in Figure 2.1. Since enthalpy and volume behave in a similar fashion, the choice of the ordinate is somewhat arbitrary. In either case, a small volume of a liquid at a temperature well above the melting temperature of that substance. As the liquid is cooled, the atomic structure of the melt will gradually change and will be characteristic of the exact temperature at which the melt is held. Cooling to any temperature below the melting temperature of the crystal would normally result in the conversion of the material to the crystalline state, with the formation of a long range, periodic atomic arrangement. If this occurs, the enthalpy will decrease abruptly to the value appropriate for the crystal. Continued cooling of the crystal will result in a further decrease in enthalpy due to the heat capacity of the crystal.

If the liquid can be cooled below the melting temperature of the crystal without crystallization, a supercooled liquid is obtained. The structure of the liquid continues to rearrange as the temperature decreases, but there is no abrupt decrease in enthalpy due to discontinuous structural rearrangement. As the liquid is cooled further, the viscosity increases. This increase in viscosity eventually becomes so great that the atoms can no longer completely rearrange to the equilibrium liquid structure, during the time allowed by the experiment. The structure begins to lag behind that which would be present if sufficient time were allowed to reach equilibrium. The enthalpy begins to deviate from the equilibrium line, following a curve of gradually decreasing slope, until it eventually becomes determined by the heat capacity of the frozen liquid, *i.e.,* the viscosity becomes so great that the structure of the liquid becomes fixed and is no longer temperature-dependent. The temperature region lying between the limits where the enthalpy is that of the equilibrium liquid and that of the frozen solid, is known as the *glass transformation region.* The frozen liquid is now a glass.

Since the temperature where the enthalpy departs from the equilibrium curve is controlled by the viscosity of the liquid, *i. e.,* by kinetic factors, use of a slower cooling rate will allow the enthalpy to follow the equilibrium curve to a lower temperature. The glass transformation region will shift to lower temperatures and the formation of a completely frozen liquid, or glass, will not occur until a lower temperature. The glass obtained will have a lower enthalpy than that obtained using a faster cooling rate. The atomic arrangement will be that characteristic of the equilibrium liquid at a lower temperature than that of the more rapidly cooled glass.

Although the glass transformation actually occurs over a temperature range, it is convenient to define a term which allows us to express the difference in thermal history between these two glasses. If the glass and supercooled liquid lines were extrapolated, they intersect at a temperature defined as the *fictive temperature.* The structure of the glass is considered to be that of the equilibrium liquid at the fictive temperature. Although the fictive temperature concept is not a completely satisfactory method for characterizing the thermal history of glasses, it does provide a useful parameter for discussion of the effect of changes in cooling rate on glass structure and properties.

As indicated above, the glass transformation occurs over a range of temperatures and cannot be characterized by any single temperature. It is, however, convenient to be able to use just such a single temperature as an indication of the onset of the glass transformation region during heating of a glass. This temperature, which is termed either the *glass transformation temperature,* or the *glass transition temperature, (TJ,* is rather vaguely defined by changes in either thermal analysis curves or thermal expansion curves. The values obtained from these two methods, while similar, are not identical. The value obtained for *T*, is also a function of the heating rate used to produce these curves. Since *T*, is a function of both the experimental method used for the measurement and the heating rate used in that measurement, it cannot be considered to be a true property of the glass. However, *T* as a useful indicator of the approximate temperature where the supercooled liquid converts to a solid on cooling, or, conversely, of which the solid begins to behave as a viscoelastic solid on heating.

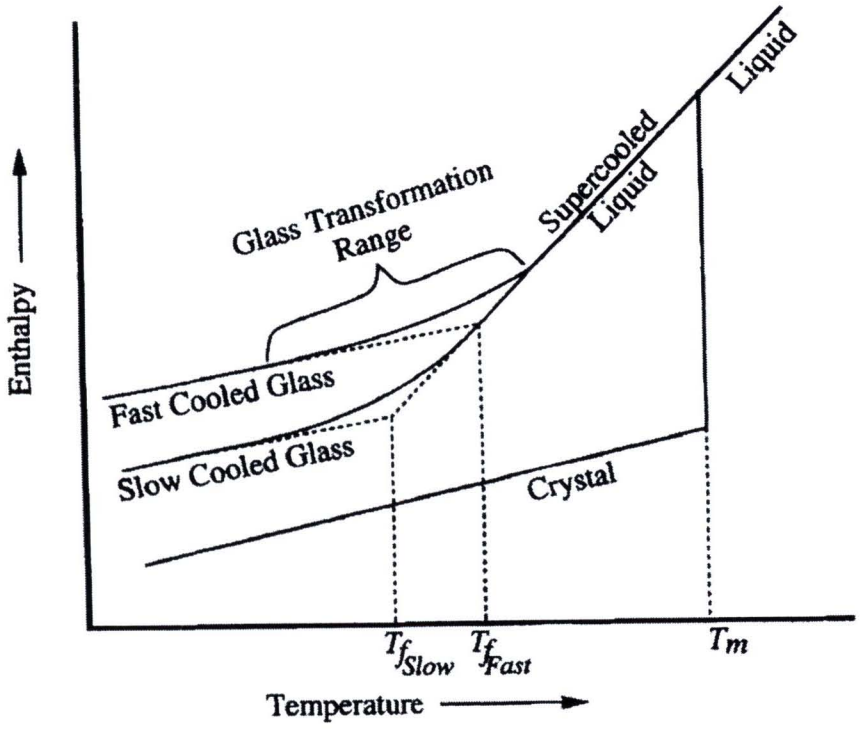

Figure 2.1 The enthalpy-temperature diagram (adapted from [52]).

2.1.4 Batch Melting Reactions

Conversion of batch to glass can be described as a process of three main stages: the first stage is characterized by the absence of any melt. In this stage, all free and most of the bonded water is removed. If water or steam are present, batch components may undergo hydrothermal reactions. Most of the crystalline inversions occur during this stage. Also, organic materials burn, reacted with oxidants, or decomposed. Solid state reactions result in development of new crystalline phases. Evolution of gases, such as water, carbon dioxide, nitrogen, or oxygen is typical.

In the second stage, the melting reactions approach equilibrium in the presence of melt. More crystalline compounds precipitate and are eventually dissolved in the melt. Inorganic salts, if they were present in the batch, melt and decompose or partially dissolve in the glass melt. All gases except refining gases are liberated. At the end of this stage, the mixture consists of a melt with suspended refractory particles and gas bubbles.

In the last stage, the remains of refractory particles are dissolved and bubbles are removed. Dissolution of particles and bubble removal, or fining, are often dealt with as two separate processes. However, since bubbles are nucleated on solid surfaces, it is convenient to think about grain dissolving and fining as one process.

2.2 Ionic Radii [53]

From quantum mechanics, atoms and ions do not have precisely defined radii. However, the concept of an ion as a hard sphere with a fixed radius is very useful when predicting crystal structure. Experimental evidence shows that such a model has some justification. Nevertheless, always bear in mind that atoms and ions are not rigid spheres and their size will be affected by their local environment. Due to the ionic radii cannot be measured directly, using X-ray crystallography so can be easily measured the ionic radii by

$$r_o = r_M + r_X \tag{2.1}$$

where r_o is the ionic radii, r_M is the radius of the cation (usually a metal) and r_X is the radius of the anion.

To obtain ionic radii it is necessary to fix the radius of one of the ions in Eq. (2.1). Historically, the radius of the I^- ions was fixed and the other radii calculated with respect to it. Later, Pauling produced a consistent set of ionic radii which has been used widely for many years. Many mineralogists use Goldschmidt's values. The most comprehensive set of ionic radii is that complied by Shannon and Prewitt and revised by Shannon. Table 2.1 lists the Shannon's ionic radii. Although there are several different tabulations they are, for the most part, internally consistent. So it is important to use radii from only one data set. Never mix values from different tabulations.

Table 2.1 Shannon's ionic radii (in pm) (adapted from [53]).

Coordination number = 6												
Ag^{+}	Al^{3+}	As^{5+}	Au^{+}	B^{3+}	Ba^{2+}	Be^{2+}	Bi^{3+}	Bi^{5+}	Br^{-}	C^{4+}	Ca^{2+}	Cd^{2+}
115	54	46	137	27	135	45	103	76	196	16	100	95
Ce^{4+}	Cl^{-}	Co^{2+}	Co^{3+}	Cr^{2+}	Cr^{3+}	Cr^{4+}	Cs^{-}	Cu^{+}	Cu^{2+}	Cu^{3+}	Dy^{3+}	Er^{3+}
87	181	75	55	80	62	55	167	77	73	54	91	89
Eu^{3+}	F^{-}	Fe^{2+}	Fe^{3+}	Ga^{3+}	Gd^{3+}	Ge^{4+}	Hf^{4+}	Hg^{2+}	Ho^{3+}	I^{-}	In^{3+}	K^{+}
95	133	78	65	62	94	53	71	102	90	220	80	138
La^{3+}	Li^{+}	Mg^{2+}	Mn^{2+}	Mn^{4+}	Mo^{3+}	Mo^{4+}	Mo^{6+}	N^{5+}	Na^{+}	Nb^{5+}	Nd^{3+}	Ni^{2+}
103	76	72	83	53	69	65	59	13	102	64	98	69
Ni^{3+}	O^{2-}	OH^{-}	P^{5+}	Pb^{2+}	Pb^{4+}	Rb^{+}	Ru^{4+}	S^{2-}	S^{6+}	Sb^{3+}	Sb^{5+}	Sc^{3+}
56	140	137	38	119	78	152	62	184	29	76	60	75
Se^{2-}	Se^{6+}	Si^{4+}	Sm^{3+}	Sn^{4+}	Sr^{2+}	Ta^{5+}	Te^{2-}	Te^{6+}	Th^{4+}	Ti^{2+}	Ti^{3+}	Ti^{4+}
198	42	40	96	69	118	64	221	56	94	86	67	61
Tl^{+}	Tl^{3+}	U^{4+}	U^{5+}	U^{6+}	V^{2+}	V^{5+}	W^{4+}	W^{6+}	Y^{3+}	Yb^{3+}	Zn^{2+}	Zr^{4+}
150	89	89	76	73	79	54	66	60	90	87	74	72
Coordination number = 4												
Ag^{+}	Al^{3+}	As^{5+}	B^{3+}	Be^{2+}	C^{4+}	Cd^{2+}	Co^{2+}	Cr^{4+}	Cu^{+}	Cu^{2+}	F^{-}	Fe^{2+}
100	39	34	11	27	15	78	58	41	60	57	131	63
Fe^{3+}	Ga^{3+}	Ge^{4+}	Hg^{2+}	In^{3+}	Li^{+}	Mg^{2+}	Mn^{2+}	Mn^{4+}	Na^{+}	Nb^{5+}	Ni^{2+}	O^{2-}
49	47	39	96	62	59	57	66	39	99	48	55	138
OH^{-}	P^{5+}	Pb^{2+}	S^{6+}	Se^{6+}	Sn^{4+}	Si^{4+}	Ti^{4+}	V^{5+}	W^{6+}	Zn^{2+}		
135	17	98	12	28	55	26	42	36	42	60		
Coordination number = 8												
Bi^{3+}	Ce^{4+}	Ca^{2+}	Ba^{2+}	Dy^{3+}	Gd^{3+}	Hf^{4+}	Ho^{3+}	In^{3+}	Na^{+}	Nd^{3+}	O^{2-}	Pb^{2+}
117	97	112	142	103	105	83	102	92	118	111	142	129
Coordination number = 12												
Ba^{2+}	Ca^{2+}	La^{3+}	Pb^{2+}	Sr^{2+}								
161	134	136	149	144								

2.3 Hybridization Orbitals in Ceramics [53]

A very important example of hybridization occurs between one s orbital and three p orbitals to form sp3 hybrid orbitals. In carbon, the ground state electron configuration is $1s^2 2s^2 2p_x^1 2p_y^1$; in this state carbon would be divalent because only the unpaired electrons in the p_x and p_y orbitals are available for bonding. To form four bonds, carbon must be raised to its valence state. This requires the promotion of one of the s electrons from the 2s orbital to the formerly empty $2p_z$ orbital. The electron configuration now becomes $1s^2 2s^1 2p_x^1 2p_y^1 2p_z^1$. This promotion costs 406 kJ/mol, but is more than compensated for by the formation of two extra C-C bonds. The C-C bond energy is 348 kJ/mol.

Hybridization between the 2s, $2p_x$, $2p_y$, and $2p_z$ orbitals occurs to form four equivalent sp^3 hybrid orbitals, as shown for carbon in Figure 2.2. Each sp^3 hybrid orbital has 25% s and 75% p character. The four sp^3 orbitals are directed toward the corners of a regular tetrahedron. Thus, in diamond each carbon atom has four localized tetrahedral sp^3 hybrid orbitals. A C-C molecular orbital (MO) is formed when orbitals from neighboring carbon atoms combine. The angle between three carbon bonds is $109^{\circ}28'$. For covalently bonded materials that show tetrahedral coordination, sp^3 hybridization must occur.

(1) Promotion of electrons to form an excited state can occur independently of hybridization.
(2) Hybridization prohibits certain configurations and allows others.
(3) The local atomic order depends upon mutual repulsion of the valence electrons and space requirements.
(4) The structure a material adopts is the one that has the lowest energy.

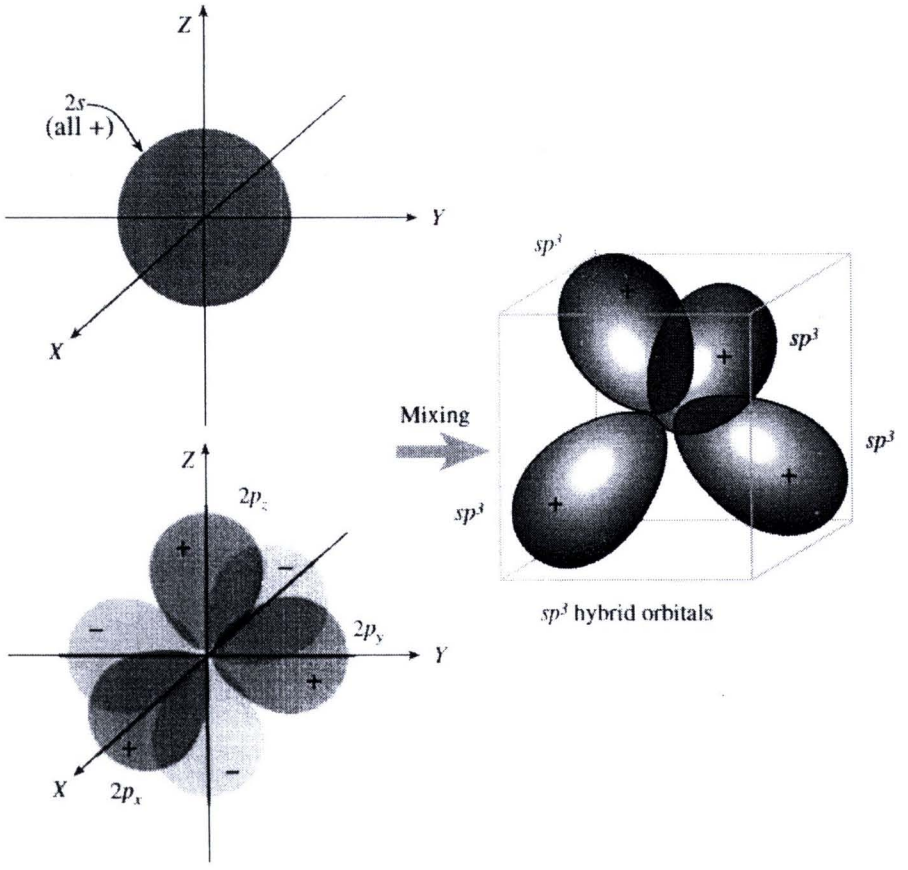

Figure 2.2 Formation of sp^3 hybrid orbitals (adapted from [53]).

In diamond, each tetrahedral group there are four sp^3 orbitals associated with the central carbon and one from each neighboring carbon, forming four bonds. The four electrons from the central carbon and one from each neighboring carbon are just sufficient to fill the bonding MOs. The four antibonding orbitals are empty. In diamond, the bonding and antibonding MOs are separated by a large energy as shown in Figure 2.3. This energy gap is the reason diamond is an electrical insulator at room temperature.

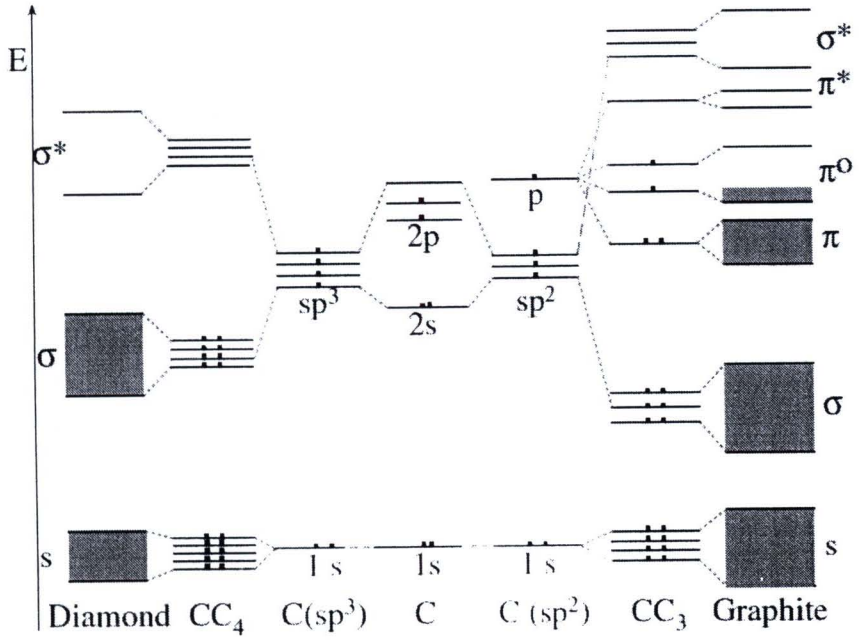

Figure 2.3 Energy level diagram for diamond and graphite (adapted from [53]).

Several other important ceramic materials in which the bonding is predominantly covalent have tetrahedral coordination of nearest-neighbor atoms, for example, silicon carbide (SiC) and aluminum nitride (AlN). In these materials sp^3 hybridization has occurred but, because of the different electronegativities of the constituent atoms, the electron density will not be symmetrical in a plane drawn between the atoms.

In graphite, the carbon atoms are in a trigonal planar arrangement with each carbon bonded to three nearest neighbors. The carbon is sp^2 hybridized. Hybridization occurs between the C 2s orbital and the $2p_x$ and $2p_y$ orbitals producing three hybrid orbitals lying in a plane at 120° to each other. Overlap of the sp^2 hybrid orbitals to produce localized bonds between carbon atoms results in a hexagonal network.

The strong bonding between carbon atoms causes overlap of adjacent $2p_z$ orbitals, which are aligned perpendicular to the plane of the hybrid orbitals. This overlap is termed π-type overlap. Since the $2p_z$ orbital is half-filled the π band will only be half full as shown in Figure 2.3. This half-filled band is why graphite has a high electrical conductivity.

In hexagonal boron nitride (h-BN), which has a structure similar to graphite, the bonding between the B and N atoms is predominantly covalent and the trigonal planar structure in the layers is a result of sp^2 hybridization of the atomic orbitals of the B and N atoms. The ground state electronic configuration of B is $1s^2 2s^2 2p_x^1$; one 2s electron is promoted to the $2p_y$ orbital giving the electron configuration $1s^2 2s^1 2p_x^1 2p_y^1$. The unfilled 2s and 2p orbitals hybridize to form three equivalent sp^2 hybrid orbitals. Nitrogen has the electronic configuration $1s^2 2s^2 2p_x p_y p_z$. Promotion of one of the 2s electrons gives the following electron configuration to the atom $1s^2 2s 2p_x 2p_y 2p_z^2$. The three half-filled orbitals combine to give three sp^2 hybrids in the *xy* plane.

The spatial arrangement of atoms around each N atom is the same as that around each B atom. Structurally there are many similarities between h-BN and graphite and both can be converted under high temperature and pressure into a cubic form. The crystal structures of cubic boron nitride (c-BN) and diamond are similar. However, unlike graphite, h-BN is an electrical insulator. The reason for this difference is that the p_z orbitals in h-BN, which lie perpendicular to the plane of the network, are either empty in the case of B or filled in the case of N. Because the energies of the p orbitals on B and N are quite different, there is little interaction, with no delocalization as was the case in graphite.

(1) h-BN is a white or colorless insulator.
(2) Graphite is a shiny black of gray electrical conductor.

Hybridization can also involve d orbitals (for atoms with $Z > 21$). The shapes produced are more complicated than those for hybridization only between s and p orbitals. Table 2.2 lists some hybrid orbitals containing s, p, and d orbitals and these are illustrated in Figure 2.4. Hybridization involving s, p, and d orbitals occurs in MoS_2. Mo ($Z = 42$) has the electron configuration [Kr] $4d^5 5s^1$. One of the 4d electrons is promoted into the empty p_x orbital to give the following electron configuration: [Kr] $4d^4 5s^1 5p_x^1$. Hybridization occurs to produce d^4sp hybrid orbitals on each Mo atom, resulting in trigonal prismatic coordination with each Mo being surrounded by six sulfur atoms. For most ceramic materials we will not need to consider hybridization involving d orbitals. However, even when they are not involved in bonding the d orbitals can be extremely important in determining the properties of materials (particularly magnetism).

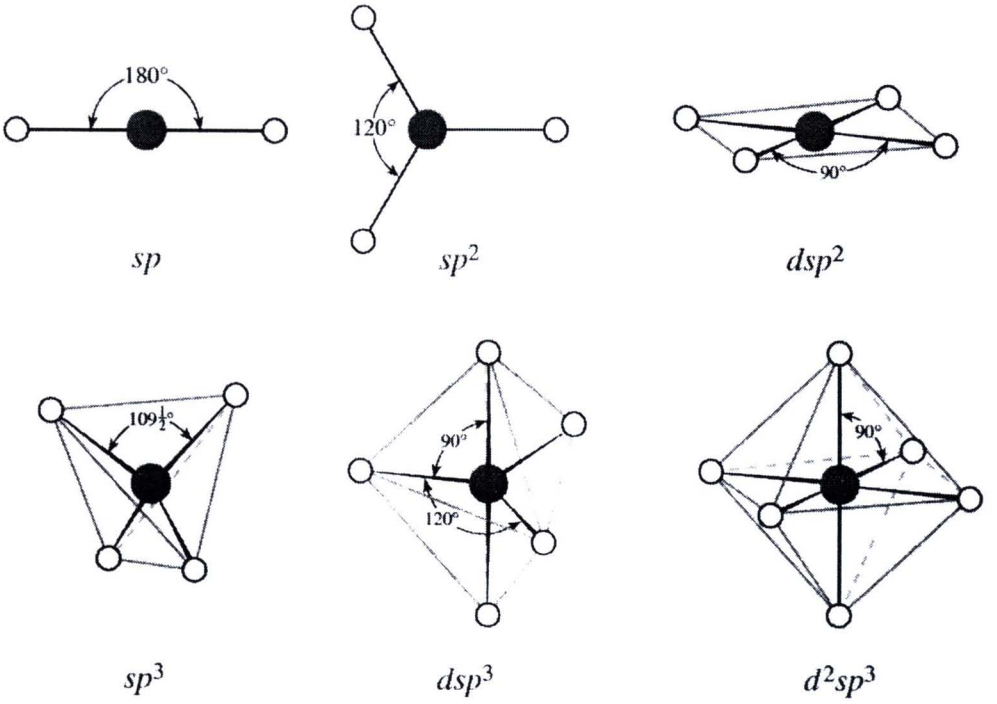

Figure 2.4 Geometric arrangements of some hybrid orbitals involving s, p and d atomic orbitals (AOs) (adapted from [53]).

Table 2.2 Orbital Geometries for hybridization (adapted from [53]).

Number of bonds	Representation	Shape	Examples
2	sp	Linear	BeH_2, $HgCl_2$
3	sp^2	Trigonal	B_2O_3, BN, graphite
4	sp^3	Tetrahedral	SiO_2, diamond
	dsp^2	Square planar	$AuBr_4$
5	dsp^3, d^3sp	Trigonal bipyramid	PCl_5
	d^2sp^2, d^4s	Square pyramid	IF_5
6	d^2sp^3	Octahedral	MoO3
	d^4sp	Trigonal prism	MoS_6 in MoS_2
8	d^4sp^3	Dodecahedral	-
	d^5p^3	Square antiprism	-

2.4 Pauling's Rules [53-54]

The structure if a crystal is determined mostly by how the atoms pack together. The same is true of binary compounds such as alloys, and of binary compounds that contain noncovalent bonds, such as ionic compounds. Ceramic materials are often thought of as being ionically bonded and ions thought of as being charged spheres. Many important ceramics are oxides in which the oxygen anion is much larger than the cation. The crystal structure adopted by the material is based on a balance between the attractive and repulsive forces in the crystal. The electrostatic attractive force between ions of unlike charge implies that an ion with a high coordination number (CN) would be more stable than an ion with a low CN, that is, the electrostatic attraction is maximized. However, if too many ions of the same charge are clustered around an individual ion of the opposite charge, they begin to interfere with one another, that is, the electrostatic repulsion is maximized. There exists a CN where the attraction is maximized and the repulsion is minimized. This number is determined by the ratio of the radii of the two ions.

In addition to the concept of electro negativity, Linus Pauling also produced a set of generalizations that are used to describe the majority of ionic crystal structures. The idea is simply that ions of opposite sign pack together in such a way as to keep ions of like sign apart.

(1) A coordinated polyhedron of anions is formed about each cation. The cation-anion distance is determined by the sum of the two radii and the CN is determined by the radius ratio.
(2) In a stable structure, the total strength of the bonds that reach an anion in a coordination polyhedron from all neighboring cations should be equal to the charge of the anion.
(3) The polyhedra in a structure tend not to share edges or faces. If the edges are shared, the shared edges are shortened. Shared faces are the least favorable.
(4) Crystals containing different cations of high valence and small CN tend not to share polyhedron elements with each other.
(5) The number of essentially different kinds of constituents in a crystal tends to be small.

Consider the two-dimensional representation of a binary ionic compound shown in Figure 2.5. The anions (open circles) are larger than the cations, and a central cation cannot remain in contact with the surrounding anions if the anion radius is larger than a certain value. Thus, the structure in Figure 2.5c is unstable, whereas the structures in Figure 2.5a and 2.5b are both stable.

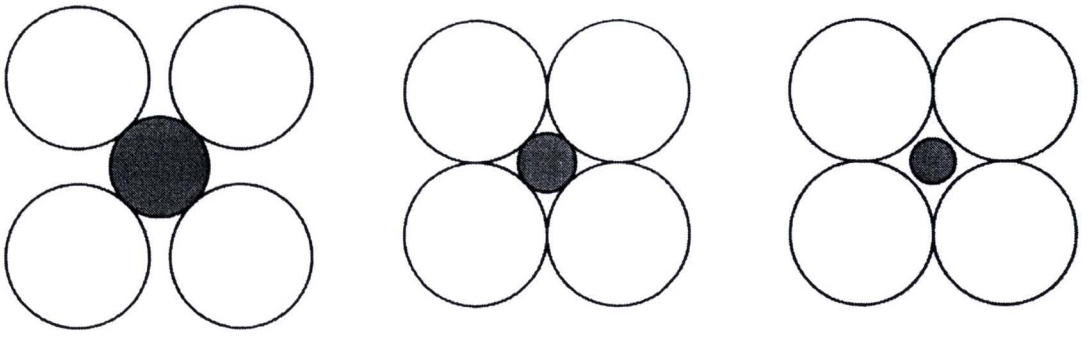

(a) (b) (c)

Figure 2.5 Coordination configurations :
(a) stable
(b) stable
(c) unstable (adapted from [54]).

The cation-anion distance is simply the sum of cation-anion radii for the stable structures. It is also true that the coordination number is determined by the radius ratio of the two ions (R_{anion}/R_{cation}). The larger the central cation, the more anions that can be packed around it. For each coordination number, there is some critical value of the radius ration which the structure will not be stable. These limits are summarized in Table 2.3.

The total of bond strength of the bonds reaching an anion from all surrounding cations is equal to the charge of anion. Pauling's third rule describes how to link these polyhedra together (Figure 2.6-2.7). Corners, rather than faces or edges, tend to be shared in stable structure. This is due to the fact that the cation separation between adjacent polyhedra decreases as edges and faces are shared, increasing repulsion and leading to unstable structures.

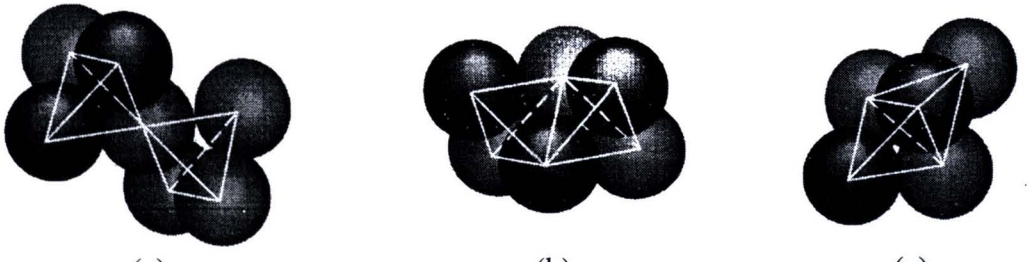

(a) (b) (c)

Figure 2.6 Tetrahedra linked by sharing :
(a) corners (b) edges (c) faces (adapted from [54]).

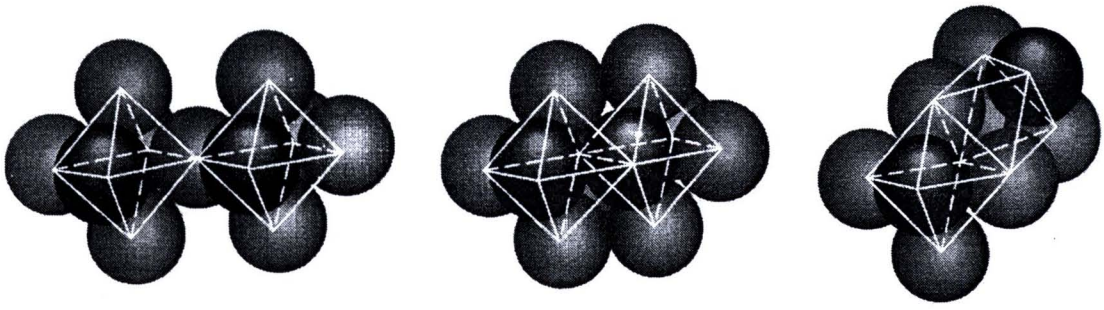

(a) (b) (c)

Figure 2.7 Octahedra linked by sharing :
(a) corners (b) edges (c) faces (adapted from [54]).

Table 2.3 Coordination number and radius ratio for various coordination numbers (adapted from [53-54]).

Coordination Number	Anion-Cation radius ratio	Coordination geometry	Polyhedron
2	6.45		Linear
3	4.45-6.45		Triangle
4	2.42-4.45		Tetrahedron
6	1.37-2.42		Octahedron
8	1.0-1.37		Cube

2.5 Glass Formation

2.5.1 Zachariasen's Rules for the Structure of Glass [53]

In 1932, W.H. Zacharaisen proposed a set of rules that is usually satisfied when an oxide forms a glass. His analysis was based on the following considerations:

(1) The interatomic bonding forces in glasses and crystals must be similar given the similar elastic modulus of the two types of solids.
(2) Like crystals, glasses consist of an extended three dimensional network, but the network does not have translational periodicity.

According to Zachariasen's rules, it has been considered that a substance can form extended three-dimensional networks lacking of periodicity with energy content comparable with that of the corresponding crystal network. These rules were remarkably successful in predicting new glass-forming oxides. The rules are as follows [55] :

(1) An oxygen atom links to not more than two cations.
(2) The number of oxygens surrounding these cations must be small.
(3) The oxygen polyhedra share with one another by their corners, not by their edges or faces.
(4) At least three corners of each polyhedra should be shared.

In a general way, the role of the cations depends on the valence, CN, and the related values of the single-bond strength. Cations of higher valence and lower coordination than the alkalis and alkaline earth oxides may also contribute, in part, to the network structure. So it can be listed the cations in three groups. The different types of ion present in oxide glasses are summarized in Table 2.4.

Table 2.4 Coordination number for glass formers, modifiers and intermediates (adapted from [53]).

Glass formers		Intermediates		Modifiers	
Dopant	CN	Dopant	CN	Dopant	CN
Si	4			Li	1
Ge	4			Na	1
B	3			K	1
Al	3	Al	3	Cs	1
P	5			Rb	1
V	5	Be	2	Be	2
As	5			Mg	2
Sb	5			Ca	2
Zr	4	Zr	4	Ba	2
				Sr	2
		Zn	2	Zn	2
		Cd	2	Cd	2
				Hg	2
				Ga	3
				Sn	4
				Pb	4

(1) Network formers are cations that form coordination polyhedra in glass.
(2) Network modifiers are oxides that do not participate directly in the network.
(3) Intermediate ions can sometimes act in either role.

Oxides, such as SiO_2, B_2O_3, P_2O_5, GeO_2 and BeF_2, are called network formers because of their ability to form branching network structures. These network formers are generally 3 to 4 in coordination numbers. Goldschmidt also considered the crystal structures and their relation to the ionic sizes, and postulated a correlation between the ability to form glass and the relative sizes of the oxygen and cation atoms. The ratios between the radius of cation (R_{cation}) and radius of anion (R_{anion}) in glass-forming oxides are in the range of about 0.2 to 0.4. The radius ratios of typical glass formers are shown in Table 2.5.

Table 2.5 Radius ratios for typical network-formers (adapted from [56]).

Compounds	Radius ratio(R_{cation}/R_{anion})
SiO_2	$R_{Si} : R_{anion} = 0.39$ Å : 1.4 Å ≈ 0.28
B_2O_3	$R_B : R_{anion} = 0.20$ Å : 1.4 Å ≈ 0.15
P_2O_5	$R_P : R_{anion} = 0.34$ Å : 1.4 Å ≈ 0.25
GeO_2	$R_{Ge} : R_{anion} = 0.44$ Å : 1.4 Å ≈ 0.31
BeF_2	$R_{Be} : R_{anion} = 0.34$ Å : 1.36 Å ≈ 0.25

2.5.2 Structural Concepts of Glass Formation

A variety of materials form glass readily by cooling from the molten state. It may be recognized that the glass formation range is quite extensive. Many other materials, on the other hand, form a noncrystalline solid only when special techniques, such as cooling from the vapor state, are used. A prime example of this is a-Si:H (amorphous hydrogenated silicon), used extensively for solar cell applications. It is not clear whether most of these amorphous solids are, in fact, glassy solids with a thermodynamic continuity to a supercooled liquid state.

The question of what characteristics make a substance a ready glass former has been the subject of intense research. Historically, the most prevalent thoughts were advanced by Zachariasen. Application of the "random network theory" concepts suggests why oxides such as SiO_2,GeO_2, and B_2O_3, where the oxygen formed tetrahedra or triangles, are ready glass formers, and why compounds such as A_2O and AO have to be ruled out. Figure 2.8 shows a two-dimensional representation of the atomic arrangements in an A_2O_3 glass versus its corresponding crystalline form. (The figure may also correspond to AO_2, where A is tetrahedrally bonded to oxygens, the fourth oxygen being out of the plane of the paper.) Whereas the local oxygen coordination is almost the same as that in a corresponding crystalline solid, the intermediate range order described by ring structures clearly differs considerably between the crystalline and the glassy forms. The glass network consists of holes that are larger than those in the crystal. (The aggregate of the holes yields the free volume discussed above.) When a compound such as Na_2O is introduced in silica, the arrangement of atoms in a two-dimensional plane is believed to look somewhat like that in Figure 2.9 Those oxygens, which connect two silicon tetrahedral at corners, are called bridging oxygens (BOs). Some oxygens are linked to only one silicon; these are called the nonbridging oxygens (NBOs). Since oxygen is a bivalent ion, its connection to only one silicon ion leaves one negative charge, which is satisfied by a univalent positive sodium ion in the interstitial spaces.

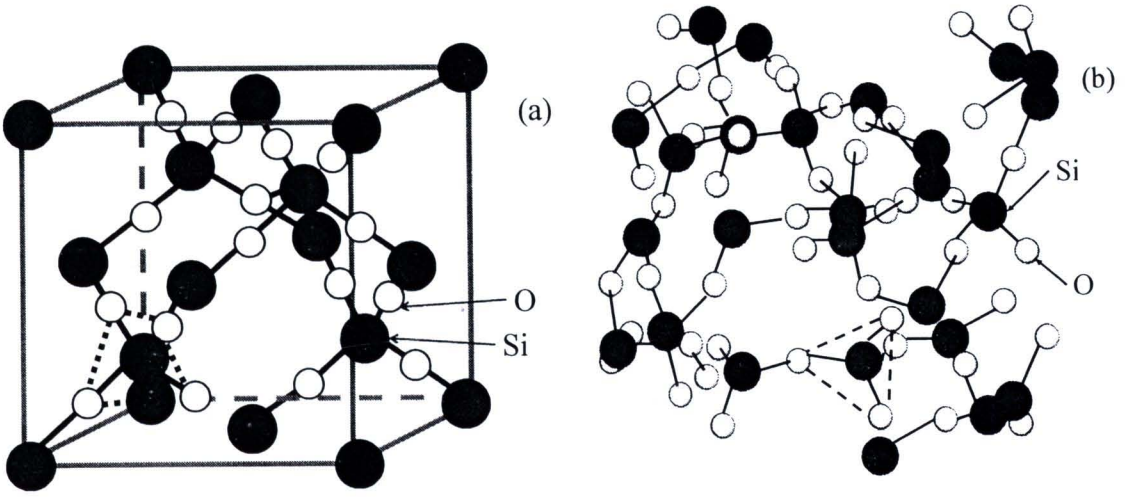

Figure 2.8 A two-dimensional representation of A_2O_3 :
(a) crystal and
(b) glass (adapted from [55]).

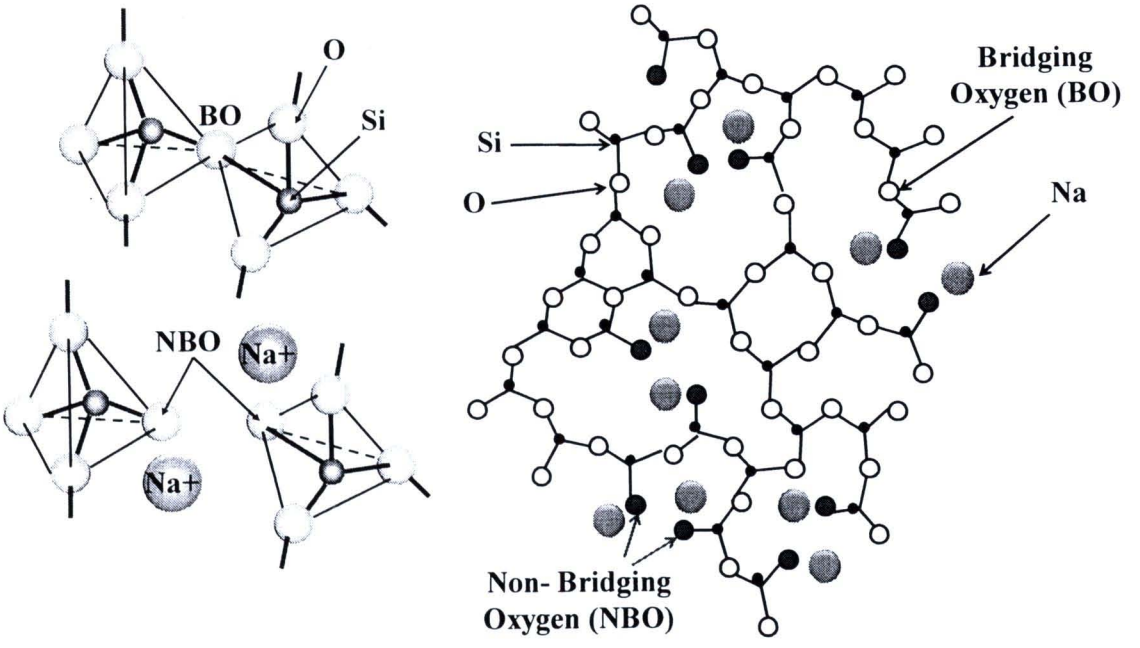

Figure 2.9 A two-dimensional representation of a sodium silicate glass (adapted from [57]).

Much of the early criticism of Zachariasen was based on the discussion of how random is random and, of course, the observation that elements such as S and Se make good glasses yet they did not fit Zachariasen's criteria. Electron microscopy of several otherwise transparent glasses has shown that glass may not be as random as Zachariasen thought and that some type of phase segregation exists in many glasses.

On the basis of the calculation of single bond strengths in an oxide AO_x, Sun suggested that oxides such as B_2O_3, SiO_2, GeO_2, P_2O_5, V_2O_5, and As_2O_5 should be classified as glass network formers (NWFs), as they ought to be able to form the glass skeleton on their own. Oxides such as Li_2O, Na_2O, K_2O, CaO, BaO, ZnO, CdO, Ga_2O3, In_2O_3, and

PbO_2 were classified as glass network modifiers (NWMs); the cations of these oxides occupied the interstitial spaces in the network formed by the NWF oxides and, hence, acted as network modifiers only. Oxides such as BeO, $A1_2O_3$, TiO_2, and ZrO_2 were termed intermediates; these did not make glass readily on their own, but did make a glass when present in large quantities mixed with the NWF or NWM oxides.

B_2O_3 normally functions as a network former in glasses. It is an important composition in special glasses which are used in electro technology, especially in the fields of heat and chemical resistance, excellent electrical insulation, low electrical loss, and gaseous impermeability. B_2O_3 will join the network structure of silica glasses without producing adverse change in the thermal expansion and durability. In the Kovar sealing, the higher percentages of B_2O_3 (17%-23%) are necessary if the glass-transition temperature of glasses must be reduced below 510°C.

2.6 Structural of B_2O_3 and Borate Glasses [39, 52]

B_2O_3 and borate glasses have been widely investigated, although their technological applications have been mostly in combination with SiO_2. B_2O_3 have the highest glass formation tendency because molten B_2O_3 does not crystallize by itself even when cooled at the slowest rate. B_2O_3 crystallizes only under pressure. Boron is the first member of the Group III in the periodic table. The size of B^{3+} is fit into the trigonal site created by 3 oxide ions in closed contact and forms a $[BO_{3/2}]$ unit. Nevertheless, B-O bond is even more covalent than the Si-O bond. $[BO_{3/2}]$ units are the primary building blocks in all borate glasses. Since B in $[BO_{3/2}]$ is electron deficient (in covalently bonded $[BO_{3/2}]$ unit, B has just 6 electrons in its outermost orbit) it can accept 2 more electrons in the form of a dative bond. This happens when an oxide ion is available in the glass composition for such additional bonding. $[BO_{4/2}]^-$ units are thus readily formed in borate glass structures. $[BO_{4/2}]^-$ units are tetrahedral. From the known covalent radii of B and O, one would expect a B-O bond distance in $[BO_{3/2}]$ unit to be 1.53 Å, which is larger than its experimentally known B-O distance of 1.38 Å. This reduction in the observed distance suggests significant back bonding from the oxygen p-orbitals to the vacant p orbital on B. Several structural studies have been performed on B_2O_3 and it may be fair to say that there is no consensus as to how the building blocks $[BO_{3/2}]$ units are connected in the structure. It is considered that boroxol ring, which consists of 3 $[BO_{3/2}]$ units in hexagonal arrangement of six V-O bonds is a major constituent of glass structure. Boroxol is particularly stable because of the possible delocalization of the electrons among the π bonded p-orbitals of B and O perpendicular to the B-O-B plane as shown in Figure 2.10. On the basis of kinetic studies using XRD, the possible stabilization energy of boroxol unit is found to be 11.8 kcal per boroxol. Glass structure is therefore considered as made up of significant proportions (80% B atoms or more) of boroxol units which are connected through simple BO_3 units. But the structural models of B_2O_3 glass, in general, fail to account for its observed low density. During modification by added ionic oxides it is suggested that one of the $[BO_{3/2}]$ units in the boroxol structure is transformed into a tetrahedral $[BO_{4/2}]^-$ unit. This destroys the planarity of the boroxol and therefore it shifts the frequency of ring rattling of boroxol from 790 cm^{-1} to 806 cm^{-1} in the Raman spectra.

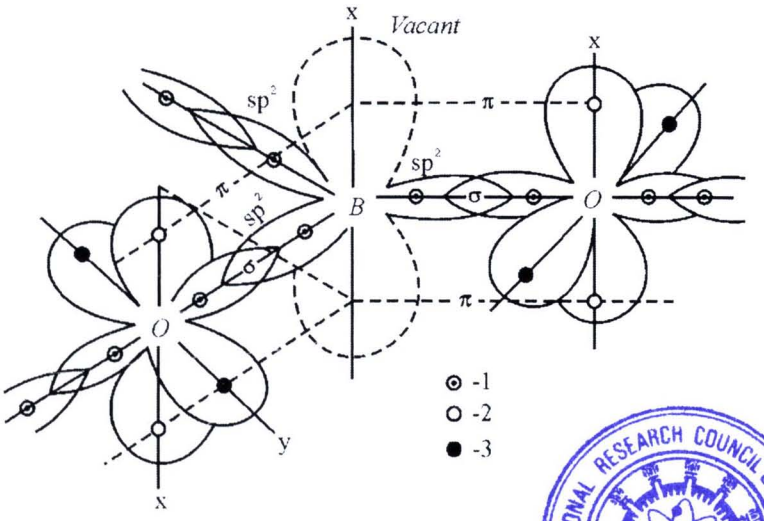

Figure 2.10 The superposition of orbitals in B_2O_3 :
(1) σ-electrons
(2) π-electrons
(3) lone pair electrons (adapted from [39]).

Vibrational spectroscopy has been used with advantage to understand the structure of borate glasses. The classic work of Krogh-Moe in 1965, indicated the possible presence of 5 different types of borate species in the glass structure (Figure 2.11). These are the species which form when B_2O_3 glass is modified by the addition of alkali or alkaline earth oxides [39]. These species are found in the modified B_2O_3 glass with alkali or alkali earth oxide.

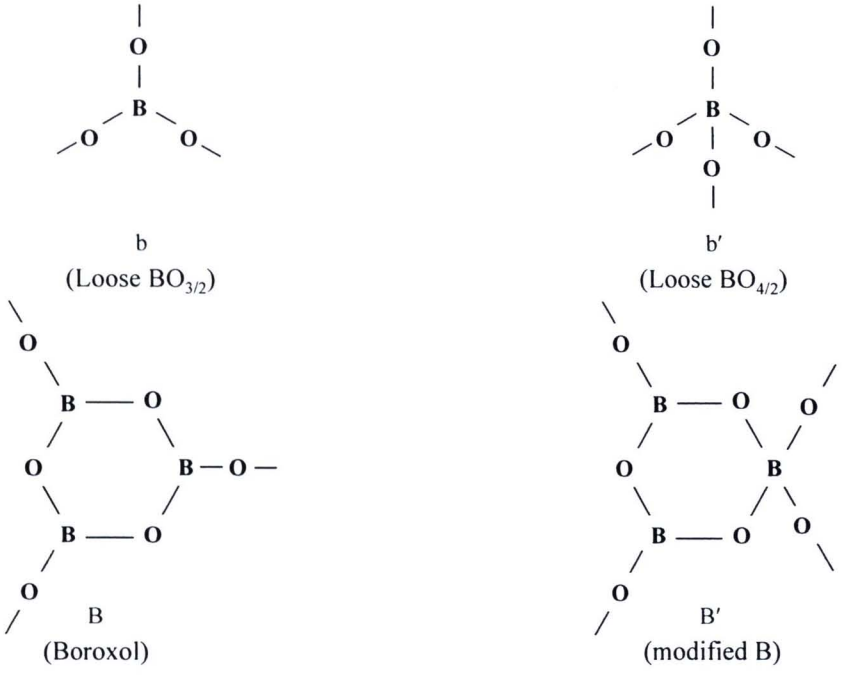

Figure 2.11 Different structural units present in alkali borate glasses (adapted from [39]).

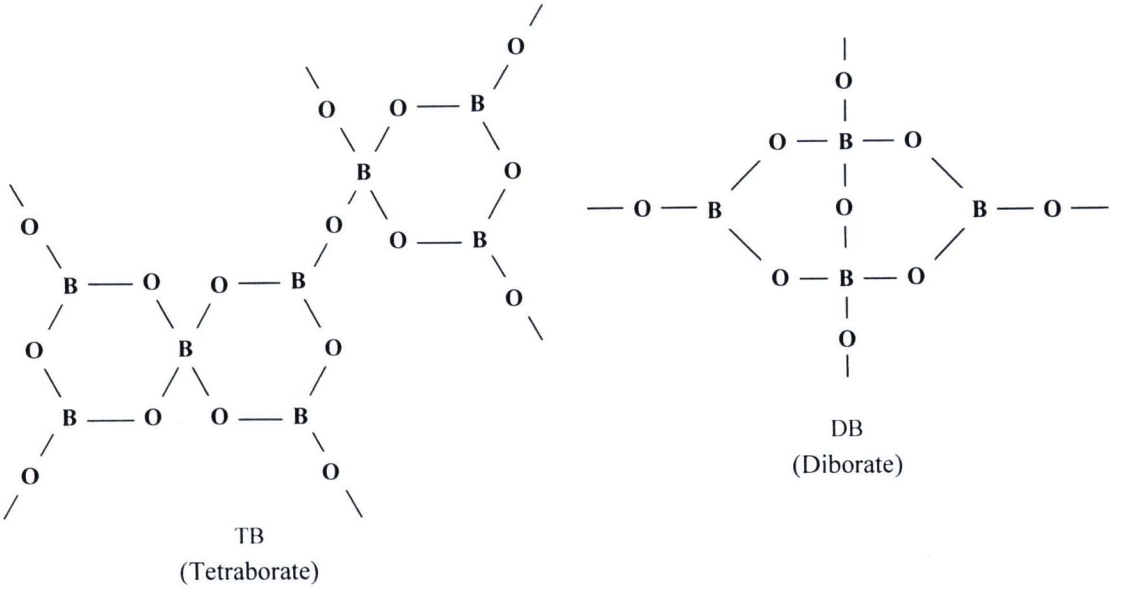

Figure 2.11 Different structural units present in alkali borate glasses (adapted from [39]) continue.

The boron ion is trivalent positive and is a glass former. The introduction of oxygen from a modifier oxide to boric oxide glass brings about one of the two possibilities [58].

(a) Create a nonbridging oxygen (NBO), as in the silicate glasses, by forming $BO_{2/2}O^-M^+$. (The "/2" subscript is denoted for the connection between a bridging oxygen and two borate ion, as shown in Figure 2.12.

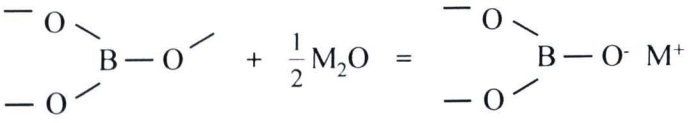

Figure 2.12 Creation of NBO when introduction of modifier to borate glass (adapted from [58]).

(b) Convert boron from a 3-coordination state ("B_3 state") to a 4-coodination state ("B_4 state"). Tetrahedral borate, B_4 is commonly found in alkali and alkali earth borate glass. (shown in Figure 2.13)

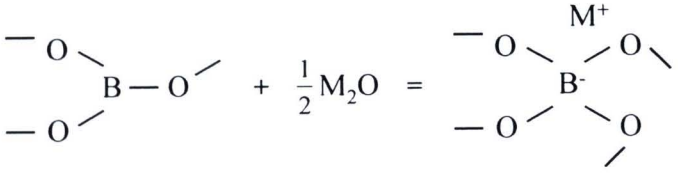

Figure 2.13 Structure change from B_3 to B_4 introduction of modifier to borate glass (adapted from [58]).

In the BO_3 group, the oxygens are fully bridging, and hence one negative charge from each oxygen satisfies the three positive charges on the boron ion. After the conversion from B_3 to B_4, all the oxygens remain bridging; the extra negative charge on the $[BO_{4/2}]^-$ group is satisfied by an alkali M^+ ion in the vicinity. The electron transfer from the M atom occurs as a distributed charge density over a large effective diameter BO_4 group, and not localized between the M atom and any specific, oxygen. Since this association is somewhat weak, the alkali ion is expected to become more mobile. However, a coulomb force in the network gives rise the increasing of the network connectivity, and hence flow-related properties (i.e., viscosity increases) and thermal expansion decrease.

In the simplest alkali borate glasses, alkali oxide initially converts the trigonal borons ($[BO_{3/2}]$ units) to tetrahedral borons ($[BO_{4/2}]^-$units) by adding O^{2-} to the trigonal boron unit [39]:

$$2[BO_{3/2}]^0 + O^{2-} \longrightarrow 2[BO_{4/2}]^-$$

$$2B_3 + O^{2-} \longrightarrow 2B_4$$

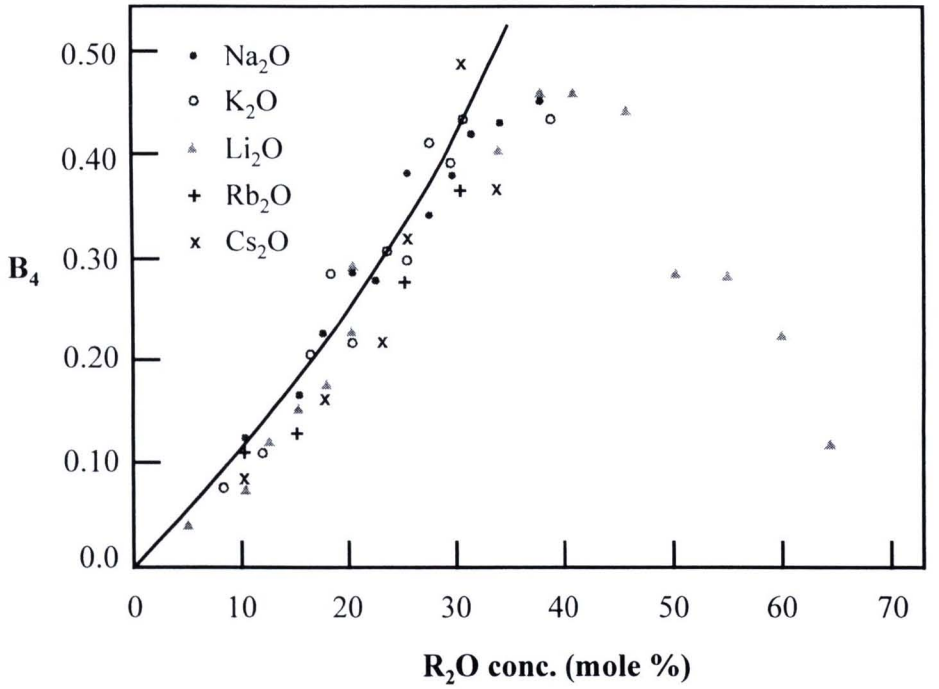

Figure 2.14 Variation of B_4 with R_2O concentration (adapted from [39]).

The formation of B_4 proceeds upon applying an amount of metal oxides until a quantity of B_4 reaches the maximum at 50%B_4 : 50%B_3. Interestingly, the quantity of B_4 is decreased when adding the metal oxide more than 50 mole%. (see Figure 2.14). The composition of B_3 and B_4 in diborate glasses is generally equal, and the corresponding mole fraction of the alkali oxide is 0.33. In Figure 2.14, the variation of B_4 (= $B_4/(B_3 + B_4)$ in various alkali borate glasses) is shown as a function of alkali oxide in mole%. The maximum of B_4 is however, depended on the size of the alkali also. In Figure 2.8 the reason for the rapid decreases in %B_4 upon further adding %R_2O is the reconversion of B_4; i.e. $B_4 \rightarrow B_3$. This has consequences on various observed properties of borate glasses and the effect has been described as 'borate anomaly'[39,59]. The tetrahedral

$[BO_{4/2}]^-$ ion is not associated with an NBO, although the unit carries a negative charge. It only means that the negative charge is spread over on all atoms in the BO_4 unit. Except in the tight structure of diborate units, two B_4 units are not directly connected to borate glasses. In lithium containing glasses, even the diborate glass does not seem to flavor $B_4 - B_4$ connections. The connectivity of the tetrahedral and the diffuse spread of the negative charge together give rise to an open structure in borate glasses for alkali oxides mole fractions < 0.33. For alkali oxide mole fractions >0.33, B_4 units breakdown and form $[BO_{1/2}O_2]^{2-}$ units [39]:

$$2[BO_{4/2}]^- + O^{2-} \longrightarrow 2[BO_{1/2}O_2]^{2-}$$

$$2B_4 + O^{2-} \longrightarrow 2B_3^{2-}$$

As a consequence, there is a network collapse and better volume utilization. Therefore, rapid reversals occur in the variation of molar volume, refractive indices, glass transition temperature (T_g), thermal expansivity etc., as a function of alkali composition. All of these variations are directly or indirectly related to energy density and are often referred as the borate anomaly. An example of the variation of some of these properties is shown in Figure 2.15.

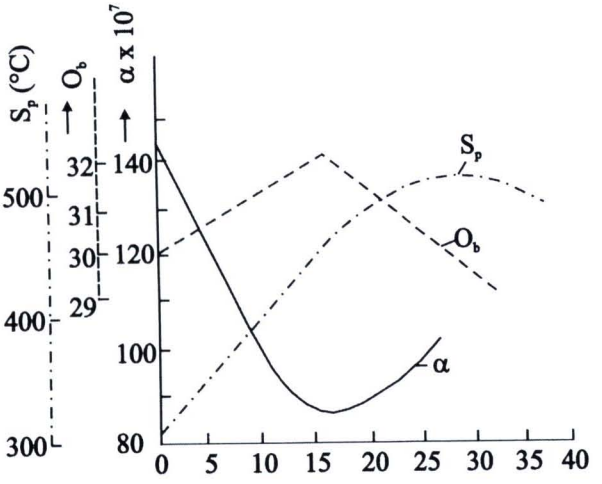

Figure 2.15 Variation in the number of bridging oxygen atoms (O_b), the coefficient of thermal expansion (α_T) and the softening temperature (S_p) as a function of alkali-oxide concentration in a B_2O_3 containing binary glass (adapted from [39]).

2.7 Density and Molar Volume [39, 60]

2.7.1 Definitions

Density of a substance is defined as the mass per unit volume, and is an intensive property. Appropriate units are g/cm^3 or g/cc (in cgs system) and kg.m^{-3} in SI system. Relative density is defined as density with respect to water 4 $^\circ$C and is, hence, unitless. Because the density is inversely proportional to the volume, a change ΔT in temperature changes the density by $-3\alpha_T \Delta T$, where α_T is the linear thermal expansion coefficient.

Since glasses may, in general, be regarded as solutions, a more useful property is the molar volume V_M, defined as the volume of one gram mole of glass, and then proceed to define partial molar volumes of the various structural units constitution the glass. The partial molar volume v_i of a species i in a solution is defined by [61]:

$$v_i = \left(\partial V / \partial n_i\right)_{n_j, T, P} \tag{2.2}$$

Therefore,

$$V_M = n_i v_i + n_j v_j \tag{2.3}$$

In essence, the total molar volume is treated as an extensive property in terms of the partial molar volumes of individual species or structural groups. The partial molar volume information can be extracted from the density data of glasses where the constituents have been systematically varied. If a Na^+ is replaced by K^+ in the glass and occupies the same interstice (without changing its size), it is clear that, although the glass density would increase because of the higher atomic weight of K^+, the partial molar volume of the alkali ion would not change. Any increase in the molar volume would be an increase in the partial molar volume of K^+ relative to Na^+. This is likely to have some relation to the relative ionic sizes of the two ions. One may readily note that, although the measurement of density changes in a family of glasses may provide only the trends, the extraction of the partial molar volumes from the density data provides further insight into structure while canceling out the effect of atomic masses.

2.7.2 Measurement of Density

Density is traditionally measure with a pycnometer, which allows the measurement of volume of a known mass of the specimen. Commercially available gas pycnometers measure the volume by measuring gass pressure changes in a compartment with and without the specimen. Using Archimedes.s principle, one may measure the specimen volume as the buoyancy (the decrease in weight) when the specimen is immersed in 4 $^\circ$C water. The buoyancy equals the weight of displaced fluid, which, for water, equals the volume in cm^3.If the glass is attacked by water, then it is advisable to use odorless kerosene as the immersion fluid, and multiply by the density of kerosene to obtain the specimen density.

Thus, if w_a is the weight of the sample in air, and w_b in water, then the buoyancy force is w_a-w_b and the density can be obtained from the following

$$\rho = w_a / \left(w_a - w_b\right) \tag{2.4}$$

Occasionally, the glass may be affected by water immersion, in which case a suitable inert liquid such as kerosene may be selected. The specimen volume in this case is given by $(w_a - w_m)/\rho_m$ where ρ_m is the density of the immersion medium. A kit supplied by scientific balance manufacturers can be utilized to obtain density measurements accurate to 0.001 g/cc. Because density can be measured readily and accurately to the third decimal place, and because it is extremely sensitive to composition, density charts are often used to control the quality of glass production in a commercial environment.

Automatic measurements of density can be carried out using pycnometers that utilize He gas as the displacement fluid. A small sample, of the order of a few milligrams, is all that is needed to make the measurement. The accuracy of such instruments is generally about 0.002 g/cc. In a manufacturing environment, a comparative density (easily accurate to 0.0002 g/cc) is more rapidly obtained using a gradient column. The gradient column consists of a vertically held long (often 1-1.5 m), glass tube with one end closed. The tube contains a liquid with a linear density gradient. To prepare the density gradient, a heavy liquid such as sym-tetrabromoethane = 2.96 g/cc) or methylene iodide (= 3.32 g/cc) is first poured into the tube, and then a lighter liquid such as isopropyl salicylate (ρ = 1.1 g/cc) is gently poured to float above the heavy liquid. With time, the liquids diffuse into each other, establishing a gradient with the help of gravity. The gradient is calibrated by allowing density standards to gently float in the column at different heights. The density of an unknown glass is obtained by reading its flotation level against a precalibrated scale placed adjacent to the column.
Another method also used commonly is the sink-float method, where the unknown specimen is gently dropped into a tube containing a slightly denser solution of organic liquids such as the ones just named. The temperature around the tube is gradually charged until the previously floating specimen begins to sink. Calibration of the liquid's density against temperature yields the density of the unknown.

2.8 Optical Basicity

The chemical interactions between the glass components are of acid-base character. The oxygen atoms in glasses behave as Lewis' bases and they can transfer part of their negative charge to the cations. The ability of oxygen to transfer the negative charges is the greatest when it is situated in the surroundings of weak cations, such as the alkalis. Duffy et al., [62-64] proposed the concept of optical basicity based on the experimental shift of the ultraviolet spectrum of a probe incorporated in various oxides. Duffy proposed a parameter Λ that permits a comparison of the acid-base character of oxides. The optical basicity Λ, of an oxidic medium, is the average electron donor power of all the oxide atoms comprising the medium. Increasing basicity results in increasing negative charge on the oxygen atoms and, thus, increasing covalency in the cation oxygen bonding.
The optical basicity could be predicted from the glass compositions and from the basicity moderating parameters of the various cations present. It is possible to calculate the so-called theoretical optical basicity of multi-component glass on the basis of the following equation proposed by Duffy and Ingram [65]:

$$\Lambda_{th} = \sum_{i=1}^{n} x_i \Lambda_i \tag{2.5}$$

where $x_1, x_2, \ldots, x_n$ are equivalent fractions of different oxides, i.e., the amount of oxygen each oxide contributes to the overall glass stoichiometry and $\Lambda_1, \Lambda_2, \ldots, \Lambda_n$ are optical basicity values assigned to the constituent oxides.

In case of the present study, the values of optical basicity for oxide have been taken from the literature [48-49]. The optical basicity evaluated for the glasses decreases when soda is replaced by one of the divalent metal oxides magnesia or barium oxide. Such low optical basicity means a reduced ability of oxide ions to transfer electrons to the surrounding cations [47].

Since the polarizability of oxide ions is closely related to the optical basicity of oxide materials, the studied glasses possess a relatively low optical basicity with the increase in the value of x. This may be understood according to the relation [66]:

$$\Lambda_{th} = 1.67\left(1 - \frac{1}{\alpha_0^{2-}}\right) \tag{2.6}$$

where α_0^{2-} is polarizability of oxide ions, and Eq. (2.6) shows that with decrease in polarizability, the optical basicity also decreases leading to a decrease in refractive index. Some theoretical values of optical basicity and related parameters for calculated of glass samples and are listed in Table 2.6 and Table 2.7, respectively [48-49].

Table 2.6 Optical basicities according to Dimitrov and Sakka calculated from refractive index ($\Lambda(n_0)$) and energy gap ($\Lambda(E_g)$), their average (Λ_{av}), optical basicity according to Duffy (Λ_{Duffy}), optical basicity according to Lebouteiller and Courtine (Λ_{LS}), and O1s binding energy (E_b) of simple oxides [49].

Oxide	$\Lambda(n_0)$	$\Lambda(E_g)$	Λ_{av}	Λ_{Duffy}	Λ_{LS}	E_b (eV)
BeO	-	-	0.375	-	0.48	-
B_2O_3	0.43	-	0.43	0.42	0.42	533.2
P_2O_5	-	-	-	0.33(0.40)	0.33	533.5
SiO_2	0.48	0.52	0.50	0.48	0.48	532.8
Al_2O_3	-	-	-	0.60	0.60	531.2
MgO	0.69	0.67	0.68	0.78	0.78	530.9
GeO_2	0.70	-	0.70	0.60	0.54	531.3
Ga_2O_3	0.71	0.80	0.755	-	-	530.6
Li_2O	0.87	-	0.87	1.00	0.48	-
CaO	1.00	0.95	0.975	1.00	1.00	529.8
Sc_2O_3	-	0.87	0.87	-	-	-
TiO_2	0.96	0.91	0.97	1.00	0.75	529.7
V_2O_5	-	1.04	1.04	-	0.63	530.0
MnO	0.94	0.96	0.95	1.00	0.96	529.8
Fe_2O_3	1.04	0.99	1.02	-	0.77	530.0
CoO	-	0.98	0.98	-	0.98	529.9
NiO	0.91	0.92	0.915	-	0.91	530.0
CuO	1.08	1.11	1.10	-	0.56	530.3
ZnO	1.03	1.13	1.08	0.95	0.92	530.3
Y_2O_3	0.99	-	0.99	-	0.72	529.3
ZrO_2	0.86	0.79	0.825	0.90	0.71	529.9
Nb_2O_5	-	1.05	1.05	-	0.61	-
MoO_3	1.07	1.07	1.07	-	0.52	530.4
In_2O_3	-	1.07	1.07	-	-	530.1
SnO_2	0.79	0.91	0.85	-	0.87	530.1
TeO_2	0.99	0.96	0.975	-	-	530.5
CeO_2	-	1.01	1.01	-	0.65	529.1
Ta_2O_5	-	0.94	0.94	-	-	-
WO_3	1.05	1.04	1.045	-	0.51	530.2
Na_2O	-	-	-	1.15	1.15	529.7
SrO	1.10	1.18	1.14	1.10	1.10	529.0
CdO	1.10	1.13	1.115	-	1.12	528.6
Sb_2O_3	1.14	1.22	1.18	-	-	-
Cs2O	-	-	-	1.70	< 1.70	529.4
BaO	1.21	1.23	1.22	1.15	1.20	528.2
PbO	1.19	1.17	1.18	0.95		529.7
Bi_2O_3	-	1.19	1.19	-	1.19	-

Table 2.7 Electronic polarizabilities of oxide ion calculated from refractive index ($\alpha_0^{2-}(n_0)$) and energy gap ($\alpha_0^{2-}(E_g)$), their average ($^{av}\alpha_0^{2-}$), and O1s binding energy (E_b) of simple oxides [49].

Oxide	α_0^{2-} (n_0) (A^3)	α_0^{2-} (E_g) (A^3)	$^{av}\alpha_0^{2-}$ (A^3)	E_b (eV)
BeO	-	-	1.290	
B_2O_3	1.345		1.345	533.2
P_2O_5	-	-	1.350	533.5
SiO_2	1.401	1.454	1.427	532.8
Al_2O_3	1.460[b]	-	1.460	531.2
MgO	1.699	1.675	1.687	530.9
GeO_2	1.720	-	1.720	531.3
Ga_2O_3	1.732	1.913	1.822	530.6
Li_2O	2.090	-	2.090	-
CaO	2.505	2.334	2.420	529.8
Sc_2O_3	-	2.075	2.075	-
TiO_2	2.368	2.188	2.278	529.7
V_2O_5	-	2.643	2.643	530
MnO	2.303	2.357	2.330	529.8
Fe_2O_3	2.647	2.467	2.557	530
CoO	-	2.405	2.405	529.9
NiO	2.202	2.218	2.210	530
CuO	2.838	2.963	2.900	530.3
ZnO	2.612	3.105	2.859	530.3
Y_2O_3	2.458	-	2.458	529.3
ZrO_2	2.054	1.897	1.975	529.9
Nb_2O_5	-	2.679	2.679	-
MoO_3	2.769	2.769	2.769	530.4
In_2O_3	-	2.762	2.762	530.1
SnO_2	1.908	2.191	2.050	530.1
TeO_2	2.444	2.358	2.401	530.5
CeO_2	-	2.522	2.522	529.1
Ta_2O_5	-	2.291	2.291	-
WO_3	2.677	2.662	2.670	530.2
SrO	2.918	3.382	3.150	529.0
CdO	2.909	3.078	2.993	528.6
Sb_2O_3	3.172	3.686	3.429	
BaO	3.652	3.830	3.741	528.2
PbO	3.450	3.311	3.381	529.7
Bi_2O_3	-	3.507	3.507	-

2.9 Photon [67-70]

A photon represents one quantum of electromagnetic energy and is treated as a fundamental particle in the Standard Model of particle physics. In this model the photon is assumed to have no rest mass. When the photon is traveling in a medium, it slows down due to interaction with the medium and acquires an effective mass. In vacuum, however, it is considered to be massless. There is no clear distinction between X-rays and gamma- rays. The term X-rays is applied generally to the photons with $E < 1$ MeV. Gammas-rays are the photons with $E \geq 1$ MeV. In what follows, the terms photon, γ , and X-rays will be used interchangeably.

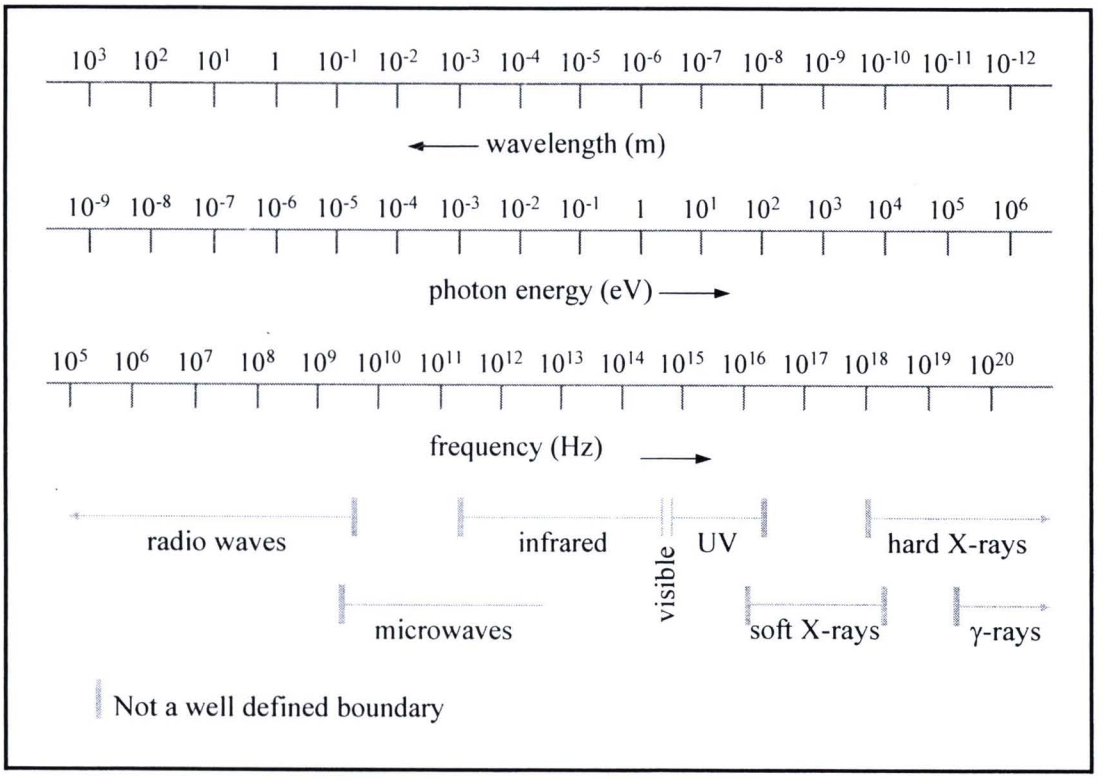

Figure 2.16 Electromagnetic spectrum (adapted from [68]).

The energy carried by a photon can be absorbed in a number of ways by other particles with which it interacts. Also, like other particles, a photon can scatter off from other particles and even experience gravitational pull.

An important property of photons is that they carry momentum even though they have no rest mass. The momentum p_γ of a photon with energy E, frequency ν, and wavelength λ is given by,

$$p_\gamma = \frac{E}{c} = \frac{h\nu}{c} = \frac{h}{\lambda} \tag{2.7}$$

2.10 Interactions of Gamma and X-Rays with Matter [67-70]

Gamma-rays are electromagnetic radiation, i.e., the release of excess energy from the nucleus of an atom retained after radioactive decay by emission of an alpha particle, but it also emits a gamma-ray at the same time. The gamma-ray emission can be simultaneous or delayed. Similarly, X-rays are electromagnetic radiation that release excess energy from the orbital electrons of an atom. Physically, gamma and X-rays are identical, with the only difference being the point of origin. Gamma-rays are also emitted during fission reactions. Unlike, alpha and beta particles, gamma-rays have no charge or mass; only kinetic energy. Therefore, their method of interaction with materials is markedly different. Instead of having Coulombic interactions with all the electrons in the material around them, gamma-rays only interact intermittently.

Although a large number of possible interaction mechanisms are known for gamma-ray in matter, only the three major types play an important role in radiation physics: the photoelectric effect, Compton scattering, and pair production. All these processes lead to the partial or complete transfer of the gamma-ray photon energy to electron energy. They result in sudden and abrupt changes in gamma-ray photon history, in that photon either disappears entirely or is scattered through a significant angle. When a gamma ray passes near an atom or electron, there is a finite probability that it will interact with that atom or electron or it may not. Gamma-ray can theoretically travel infinite distances without interacting at all.

2.10.1 Compton Scattering or Compton Effect

The interaction process of Compton scattering takes place between the incident photon and a free electron. In the collision, a portion of the gamma-ray's energy is transferred to the electron. Of course, under normal circumstances, all the electrons in a medium are not free but bound. If the energy of the photon, however, is of the order of keV or more, while the binding energy of the electron is of the order of eV, the electron may be considered free. This process is most often the predominant interaction mechanism for gamma-ray energies typical of radioisotope sources.

Figure 2.17 depicts an incoming gamma ray, E_γ, colliding with an electron and departing with reduced energy, $E_{\gamma'}$, and the electron has the remainder of the energy as kinetic energy. The original gamma ray is reduced in energy but continues on until it has another collision (only its direction of motion and energy change). Therefore, conservation of energy gives (assuming the electron is stationary before the collision) [67]:

$$T_e = E_\gamma - E_{\gamma'} \tag{2.8}$$

where T_e, E_γ *and* $E_{\gamma'}$ are kinetic energy of the electron, incident photon energy and scattered photon energy, respectively.

If Eq. (2.8) is used along with the conservation of momentum equations, the energy of the scattered photon as a function of the scattering angle θ can be calculated. The result is [66]:

$$E_{\gamma'} = \frac{E_\gamma}{1+(1-\cos\theta)E_\gamma / mc^2} \tag{2.9}$$

Using Eq. (2.8) and Eq. (2.9), one obtains the kinetic energy of the electron.

$$T_e = \frac{(1-\cos\theta)E_\gamma / mc^2}{1+(1-\cos\theta)E_\gamma / mc^2} E_\gamma \tag{2.10}$$

A matter of great importance for radiation measurement is the maximum and minimum energy of the photon and the electron after the collision. The minimum energy of the scattered photon is obtained when $\theta = \pi$ this, of course, corresponds to the maximum energy of the electron. From Eq. (2.9):

$$E_{\gamma',min} = \frac{E_\gamma}{1+2E_\gamma / mc^2} \tag{2.11}$$

and

$$T_{e,max} = \frac{2E_\gamma / mc^2}{1+2E_\gamma / mc^2} E_\gamma \tag{2.12}$$

The maximum energy of the scattered photon is obtained for $\theta = 0$, which essentially means that the collision did not take place. From Eq. (2.8) :

$$E_{\gamma',max} = E_\gamma \tag{2.13}$$

$$T_{e,\min} = 0 \tag{2.14}$$

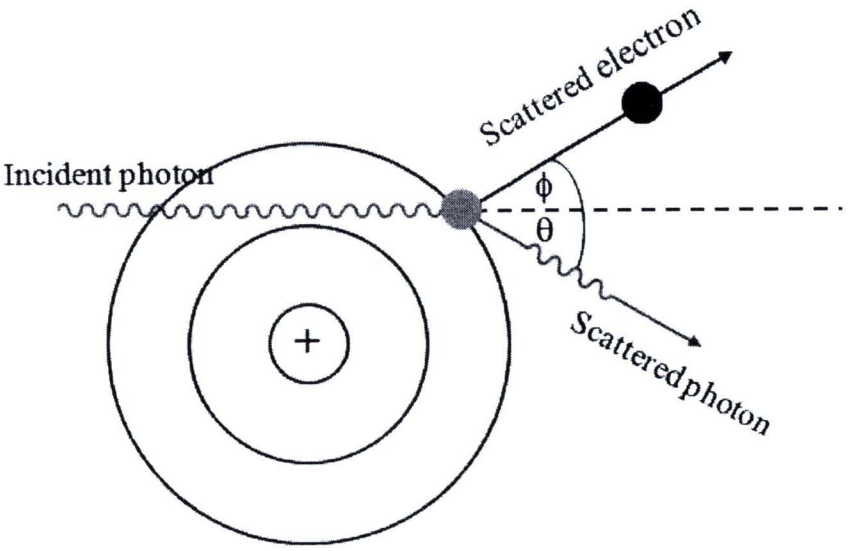

Figure 2.17 The Compton effect (adapted from [67]).

The conclusion to be drawn from Eq. (2.13) is that the minimum energy of the scattered photon is greater than zero. Therefore, in Compton scattering, it is impossible for all the energy of the incident photon to be given to the electron. The energy given to the electron will be dissipated in the material within a distance equal to the range of the electron. The scattered photon may escape.

The probability that Compton scattering will occur is called the Compton coefficient or the Compton cross section. It is a complicated function of the photon energy, but it may be written in the form [67]:

$$\sigma(m^{-1}) = NZf(E_\gamma) \tag{2.15}$$

where σ is the probability for Compton interaction to occur per unit distance, $f(E_\gamma)$ is a function of E_γ. If one writes the atom density N explicitly, Eq. (2.15) takes the form:

$$\sigma \sim \rho\frac{N_A}{A}Zf(E_\gamma) \sim \rho\left(\frac{N_A}{A}\right)\frac{A}{2}f(E_\gamma) \sim \rho\frac{N_A}{2}f(E_\gamma) \tag{2.16}$$

In deriving Eq. (2.16), use has been made of the fact that for most materials, except hydrogen, $A \approx 2Z$ to $A \approx 2.6Z$. According to Eq. (2.16), the probability for Compton scattering to occur is almost independent of the atomic number of the material. In Figure 2.18 shows how π changes as a function of E_γ and Z. If the Compton cross section is known for one element, it can be calculated for any other by using Eq. (2.15) (for photons of the same energy):

$$\sigma_2(m^{-1}) = \sigma_1\left(\frac{\rho_2}{\rho_1}\right)\left(\frac{A_1}{A_2}\right)\left(\frac{Z_2}{Z_1}\right) \tag{2.17}$$

where σ_1 and σ_2 are given in m^{-1}. If σ_1 and σ_2 are given in m^2/kg, Eq. (2.17) takes the form:

$$\sigma_2(m^2/kg) = \sigma_1\left(\frac{A_1}{A_2}\right)\left(\frac{Z_2}{Z_1}\right) \tag{2.18}$$

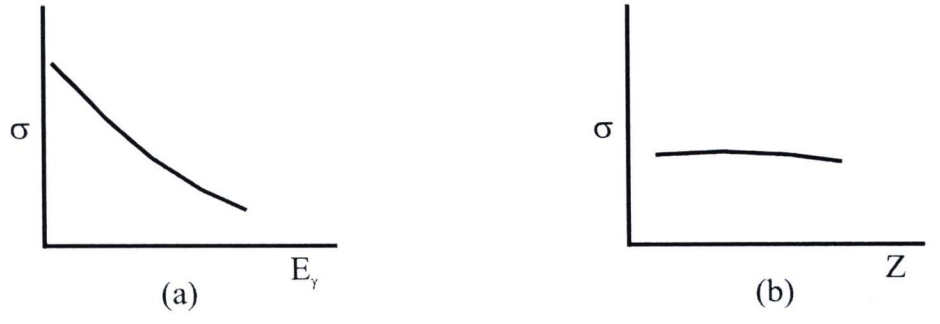

Figure 2.18 Dependence of the Compton cross section on (a) photon energy (b) atomic number of the materials (adapted from [67]).

For Compton effect can be summarized as follows:

- A Compton interaction occurs between a photon and a "free" electron producing a recoiling electron and a scattered photon of reduced energy.
- Kinetic energy transferred to the electron is directly proportional to the scattering angle of the scattered photon and, on average, increases with photon energy.
- The Compton interaction coefficient decreases with increasing energy and is almost independent of atomic number.

2.10.2 Photoelectric Effect

In photoelectric effect, a photon undergoes an interaction with a bound atomic electron and eject it from the atom, occurs when a gamma ray is absorbed by an electron and the kinetic energy of the gamma ray is transferred to the electron. As a result of the interaction, the photon completely disappears and one of the atomic electrons is ejected as a free electron, called the photoelectron. Figure 2.19 depicts an incoming gamma-ray being absorbed by an electron which then shoots off with a kinetic energy equal to the incoming gamma-rays energy minus the binding energy of the electron to the atom. The original gamma ray has been stopped and eliminated and replaced by an photoelectron which its kinetic energy, T_e is

$$T_e = E_\gamma - B.E. \tag{2.19}$$

where E_γ is energy of the incident photon
$B.E.$ is binding energy of electron

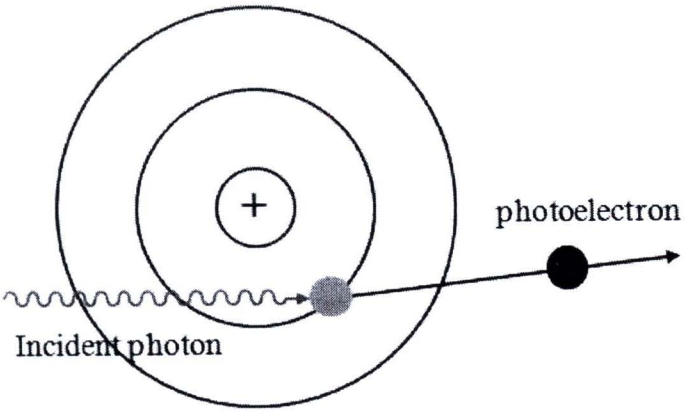

Figure 2.19 The Photoelectric effect (adapted from [67]).

The photoelectric process is the predominant mode of interaction for gamma or X-rays of relatively low energy. The probability of this interaction occurring is called the photoelectric cross-section or photoelectric coefficient, τ, increases rapidly with atomic number of the target atom. In addition, it also has a strong. It is a function of the atomic number (Z) of the absorbing material (generally related to the density ρ of the absorbing medium), gamma rays energy (E_γ). The equation giving τ may be written as [67]:

$$\tau\left(m^{-1}\right) = aN\frac{Z^n}{E_\gamma^m}\left[1-\theta(Z)\right] \tag{2.20}$$

where τ is probability for photoelectric effect to occur per unit distance traveled by the photon
a is constant, independent of Z and E_γ
m,n is constants with a value of 3 to 5 (their value depends on E_γ)
N is number of atom/m^3

The term in parentheses indicates correction terms of the first order in Z. Figure 2.20 shows how the photoelectric coefficient changes as a function of E_γ and Z. As Figure 2.19 and Eq. (2.20) show, the photoelectric effect is more important for high-Z material, i.e., more probable in Pb (Z = 82) than in Al (Z = 13). It is also more important for E_γ = 10 keV than E_γ = 500 keV (for the same material).

Using Eq. (2.20), one can obtain estimates of the photoelectric coefficient of one element in terms of that of another. If one takes the ratio of τ for two elements, the result for photons of the same energy is [67]:

$$\tau_2\left(m^{-1}\right) = \tau_1 \frac{\rho_2}{\rho_1}\left(\frac{A_1}{A_2}\right)\left(\frac{Z_2}{Z_1}\right)^n \tag{2.21}$$

where ρ and A represent the density and atomic weight, respectively, of the two elements, and τ_1 and τ_2 are given in m^{-1}. If τ_1 and τ_2 are given in m^2/kg, Eq. (2.21) takes the form [65]:

$$\tau_2\left(m^2/kg\right) = \tau_1 \frac{A_1}{A_2}\left(\frac{Z_2}{Z_1}\right)^n \tag{2.22}$$

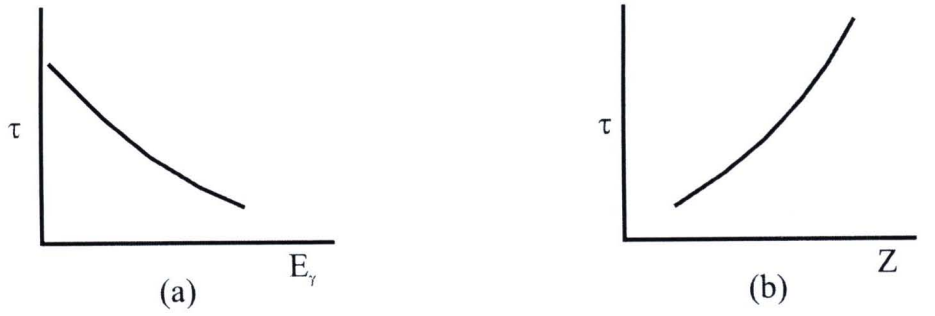

Figure 2.20 Dependence of the photoelectric cross-section on (a) photon energy and (b) atomic number of the material (adapted from [67]).

The photoelectric effect can be summarized as follows:

- It occurs only with bound electrons because the entire atom is necessary to conserve momentum.
- The interaction coefficient is greatest when the photon energy just equals the amount to overcome the binding energy of the orbital electron, causing it to be ejected from its shell.
- The photoelectric absorption coefficient is directly proportional to Z^5 and inversely proportional to E_γ^3 on average.

2.10.3 Pair Production

Pair production is an interaction occurs when the photon energy exceeds twice the rast mass energy of an electron (1.02 MeV), the process of pair production is energetically possible. As a result of the interaction, the photon disappears and an electron-positron pair appears (Figure 2.21). Although the nucleus does not undergo any change as a result of this interaction, its presence is necessary for pair production to occur. A gamma-ray will not disappear in empty space by producing an electron-positron pair.

Conservation of energy gives the following equation for the kinetic energy of the electron and the positron:

$$T_{e^-} + T_{e^+} = E_\gamma - (mc^2)e^- - (mc^2)e^+ = E_\gamma - 1.022 \text{ MeV} \tag{2.23}$$

Pair production may take place in the field of an electron. The probability for that to happen is much smaller and the threshold for the threshold for the gamma energy is $4mc^2 = 2.04$ MeV.

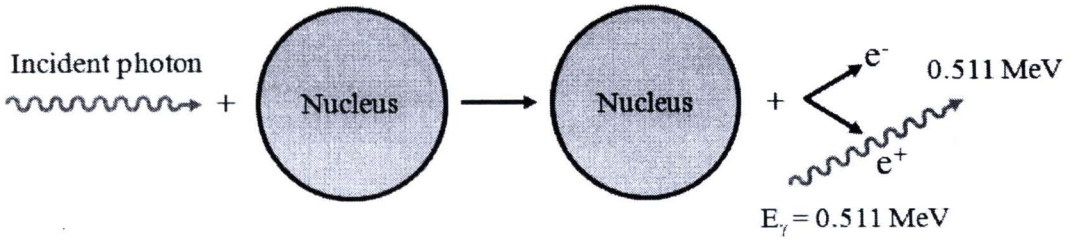

Figure 2.21 Pair production. The gamma disappears and a positron-electron pair is created. Two 0.511 MeV photons are produced when the positron annihilates (adapted from [67]).

The available kinetic energy is equal to the energy of the photon minus 1.022 MeV, which is necessary for the production of the two rest masses. Electron and positron share, for all practical purposes, the available kinetic energy, i.e.:

$$T_{e^-} = T_{e^+} = \frac{1}{2}(E_\gamma - 1.022 \text{ MeV}) \tag{2.24}$$

Pair production eliminates the original photon, but two photons are created when the positron annihilates. The annihilation gammas are important in constructing shielding against them as well as for the detection of gammas.

The probability for pair production to occur, called the pair production coefficient or cross section, is proportional to the square of the atomic number Z for photons with energy greater than 2 x 0.511 MeV. It may be written in the form:

$$\kappa(m^{-1}) = NZ^2 f(E_\gamma, Z) \tag{2.25}$$

where κ is the probability for pair production to occur per unit distance traveled and $f(E, Z)$ is a function, which change slightly with Z and increases with E_γ.

In Figure 2.22 shows how κ changes with E_γ and Z. It is important to note that κ has a threshold at 1.022 MeV and increases with E_γ and Z. Of the three coefficients (τ and π being the other two), κ is the only one increasing with the energy of the photon.

If the pair production cross-section is known for one element, an estimate of its value can be obtained for any other element by using Eq. (2.25) (for photons of the same energy):

$$\kappa_2\left(m^{-1}\right) = \kappa_1\left(\frac{\rho_2}{\rho_1}\right)\left(\frac{A_1}{A_2}\right)\left(\frac{Z_2}{Z_1}\right)^2 \tag{2.26}$$

where κ_1 and κ_2 are given in m^{-1}.

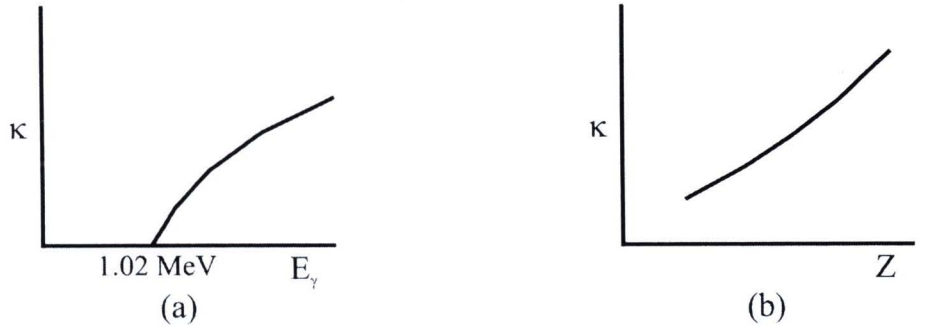

Figure 2.22 Dependence of the pair-production cross section on (a) photon energy and (b) atomic number of the material (adapted from [67]).

Pair production can be summarized as follows:

- They occur for photons with $E_\gamma \geq 1.022$ MeV primarily in the field of the nucleus to produce two electron masses with kinetic energy, but can also occur with an orbital electron yielding a triplet of electron masses.
- The kinetic energy shared between the positron and the electron is E_γ -1.022 MeV.
- The positron annihilates with a free electron after dissipating its kinetic energy to produce two 0.511 MeV annihilation photons.
- The absorption coefficient increases rapidly with energy above the 1.022 MeV threshold and varies approximately as Z^2.

2.11 Gamma-Ray Attenuation Coefficient [67-70]

When a photon penetrates through matter, it may interact through any of the three major interactions discussed earlier. (For pair production, E_γ >1.022 MeV.). There are other interactions, but they are not mentioned here because they are not important in the detection of gamma-rays.

Figure 2.23 shows the relative importance of the three interactions as E_γ and Z change. Consider a photon with E = 0.1 MeV, if this particle travels in carbon (Z = 6), the Compton effect is the predominant mechanism by which this photon interacts. If the same photon travels in iodine (Z = 53), the photoelectric interaction prevails. For a γ of 1MeV, the Compton effect predominates regardless of Z. If a photon of 10 MeV travels in carbon, it will interact mostly through Compton scattering. The same photon moving in iodine will interact, mainly, through pair production.

The total probability for interaction per unit path length μ, called the total linear attenuation coefficient, is equal to the sum of the three probabilities:

$$\mu = \tau\,(photoelectric) + \tau\,(Compton) + \kappa\,(pair) \tag{2.27}$$

where μ is the probability of interaction per unit distance.

There are tables that give μ for all the elements, for many photon energies. Most of the tables provide μ in units of m^2/kg. (or cm^2/g), because in these units the density of the material does not have to be specified.

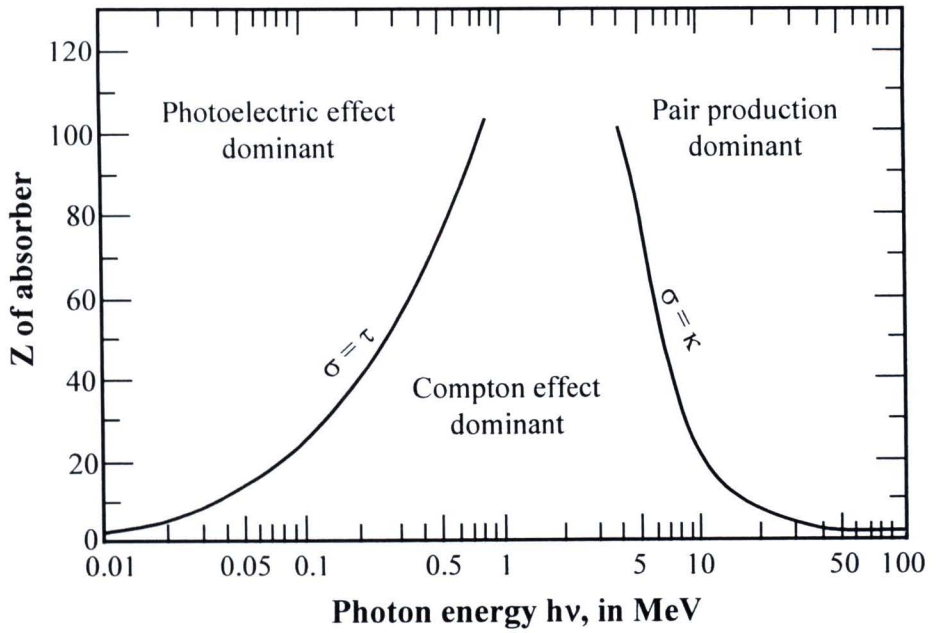

Figure 2.23 The relative importance of the three major gamma interactions (adapted from [70]).

The total linear attenuation coefficient in the above relations determines how quickly or slowly a certain photon beam will attenuate while passing through a material. It is a function not only of the photon energy but also of the type and density of the material. Therefore, the mass attenuation coefficient, μ_m, is much more widely uses is defined:

$$\mu_m = \frac{\mu}{\rho} \tag{2.28}$$

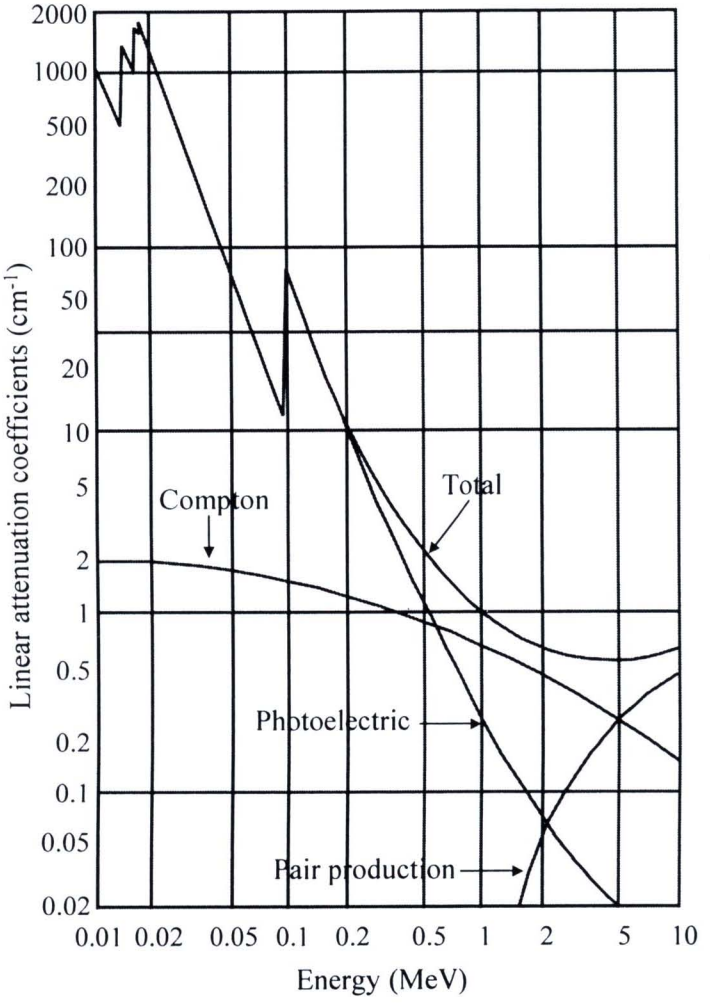

Figure 2.24 Mass attenuation coefficients for lead ($Z = 82$, $\rho = 11.35 \times 10^3$ kg/m^3) (adapted from [70]).

Figure 2.24 shows the individual coefficients as well as the total mass attenuation coefficient for lead, as a function of photon energy. The total mass attenuation coefficient shows a minimum because as E increases, τ decreases, κ increases, and σ does not change appreciably. However, the minimum of μ does not fall at the same energy for all elements. For lead, μ is minimized at $E_\gamma \sim 3.5$ MeV; for aluminum, the minimum is at 20 MeV; and for NaI, the minimum is at 5 MeV.

2.11.1 Measuring Attenuation Coefficients

If a parallel beam of monoenergetic gamma-rays goes through a material of thickness x, the fraction of the beam that traverses the medium without any interaction is equal to $e^{-\mu x}$ (see Figure 2.25). The probability that a photon will go through thickness x without an interaction is:

$$I = I_0 e^{-\mu x} \tag{2.29}$$

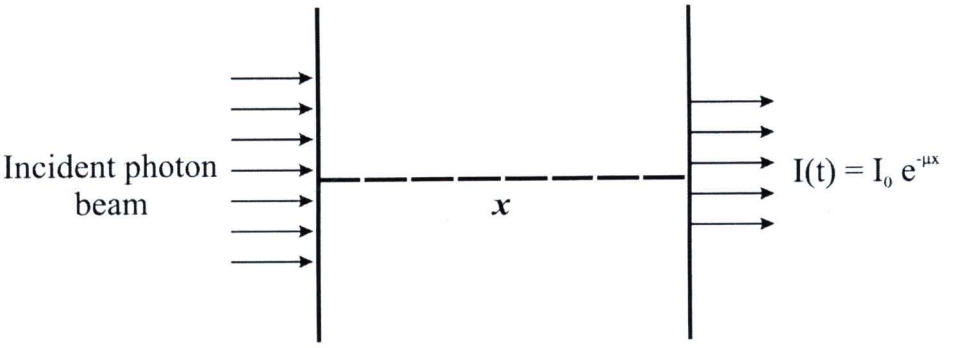

Figure 2.25 The intensity of the transmitted beam (only particles that did not interact) decreases exponentially with material thickness (adapted from [67]).

As particles pass through material, they undergo collisions that may change their direction of motion. The average distance between these collisions is therefore a measure of the probability of a particular interaction. This distance, generally known as the mean free path (*MFP*), that is

$$MFP = \frac{\int_0^\infty x e^{-\mu x} dx}{\int_0^\infty e^{-\mu x} dx} = \frac{1}{\mu} \tag{2.30}$$

Thus, the mean free path is simply the inverse of the total linear attenuation coefficient. If $\mu = 10\ m^{-1}$ for a certain γ-ray traveling in a certain medium, then the distance between two successive interactions of this gamma in that medium is $MFP = 1/\mu = 1/10\ m = 0.10\ m$.

2.11.2 Mixture and Compounds

The attenuation coefficient of a compound or mixture at a certain energy can be obtained by simply taking the weighted mean of its individual components according to The total mass attenuation coefficient for a compound or a mixture is calculated by: [44, 67]

$$\mu_m = \sum_{i=1}^{n} w_i (\mu_m)_i \tag{2.31}$$

where μ_m is total mass attenuation coefficient for a compound or a mixture
w_i is weight fraction of i^{th} element in the compound
$(\mu_m)_i$ is total mass attenuation coefficient of i^{th} element

2.12 Effective Atomic Numbers and Effective Electron Density

In this section we summarize theoretical relations used in the present work. A parallel beam of monoenergetic gamma-ray photons is attenuated in matter according to the Lambert-Beer law [67]:

$$I = I_0 \exp(-\mu_m \rho x) \tag{2.32}$$

where I_0 and I are incident and transmitted intensities of gamma radiation, respectively. μ_m is the mass attenuation coefficient for absorber, x is the thickness of absorber and ρ is the density of absorber.

Theoretical values of the mass attenuation coefficients of mixture or compound have been calculated by WinXCom, based on the mixture rule from Eq. (2.31).

This mixture rule is valid when the effects of molecular binding, chemical and crystalline environment are negligible. The values of mass attenuation coefficients can be used to determine the total atomic cross-section ($\sigma_{t,a}$) by the following relation [34]:

$$\sigma_{t,a} = \frac{(\mu_m)}{N_A \sum_{i}^{n} (w_i / A_i)} \tag{2.33}$$

where N_A is Avogadro's number, A_i is atomic weight of the constituent element of mixture . Also the total electronic cross-section ($\sigma_{t,el}$) for the element is expressed by the following formula [34]:

$$\sigma_{t,el} = \frac{1}{N_A} \sum_{i}^{n} \frac{f_i A_i}{Z_i} (\mu_m)_i \tag{2.34}$$

where f_i is the number of atoms of the element i^{th} relative to the total number of atoms of all elements in mixture, Z_i is the atomic number of the i^{th} element in alloy.

Atomic number, Z, is and ubiquitous parameter in atomic and nuclear physics where it occurs in almost any formula. For a complex medium, the effective atomic number, Z_{eff}, is a convenience parameter for representing gamma and X-ray interactions. However, a single number cannot represent the effective atomic number of a material, which s composed of several elements. Accordingly, Z_{eff}, is no true constant for a given material, but a parameter varying with photon energy with photon energy depending on the interaction processes involved. The effective atomic number is closely related to the electron density, express in number of electron per unit mass.

By using the mass attenuation coefficient of mixture, the effective atomic number (Z_{eff}) and the effective electron density (N_e) (number of electrons per unit mass) were determined from Eq. (2.33) and Eq. (2.34), respectively [34]:

$$Z_{eff} = \frac{\sigma_{t,a}}{\sigma_{t,el}} \tag{2.35}$$

Finally, the effective number, N_e, of electrons per unit mass of the absorber can be found from

$$N_e = \frac{\mu_m}{\sigma_{t,el}} \tag{2.36}$$